GEOSPATIAL ANALYSIS OF POTENTIAL FLOODING FROM STORM SURGE AND SEA-LEVEL CHANGE ON THE TEXAS COAST BY 2100

by

GENNADII PRYKHODKO

THESIS

Submitted in partial fulfillment of the requirements
for the degree of Master of Science in Earth and Environmental Sciences at
The University of Texas at Arlington
May, 2020

Arlington, TX

Supervising Committee:

Arne M. E. Winguth, Supervising Professor
Taylor M. Hughlett
Hyeong-Moo Shin

ACKNOWLEDGEMENTS

I would first like to thank my supervising professor, Dr. Arne Winguth, of the Earth and Environmental Sciences Department at the University of Texas at Arlington. Dr. Winguth spent many hours assisting me, answering with my thesis related questions and addressing technical issues I encountered during my graduate career. He challenged me, encouraged me to grow my skills, and gave me freedom to explore different areas of my research. Without Dr. Winguth's support, I would not have been able to accomplish this important milestone in my life.

I would like to thank my two other committee members, Dr. Hyeong-Moo Shin and Dr. Taylor Hughlett, without whom this research would be much harder. Dr. Shin was helpful to answer statistical questions related to my research. Dr. Hughlett donated much of her time to answer my questions and address concerns I had about my research. Her support, experience and expertise in climate science helped me succeed in the program.

I would like to acknowledge high-performance computing support from Cheyenne (doi:10.5065/D6RX99HX) provided by NCAR's Computational and Information Systems Laboratory, sponsored by the National Science Foundation.

April 29, 2020

TABLE OF CONTENTS

LIST OF ILLUSTRATIONS

LIST OF TABLES

ABSTRACT

GEOSPATIAL ANALYSIS OF POTENTIAL FLOODING FROM STORM SURGE AND SEA-LEVEL CHANGE ON THE TEXAS COAST BY 2100

Gennadii Prykhodko, MS

The University of Texas at Arlington, 2020

Supervising Professor: Arne M. E. Winguth

Tropical cyclones pose a major hazard to the State of Texas. Anthropogenic climate change and global warming have the potential to increase extreme weather events and lead to enhanced flood hazard zones. This study aims to analyze potential flooding from hurricane induced storm tides in the Houston metroplex area, and particularly in Harris County. A geospatial framework is proposed for modeling inundation from storm surge with sea-level rise. Spatial models and statistics are applied to the State of Texas with the focus on the Houston metropolitan area including Harris County. Historical and observational tropical cyclone data is used to examine past storm events and to construct spatial distribution models. Climatology of tropical cyclones reveals increasing rates of hurricanes Category 3 and higher in the Atlantic basin. Spatial modeling of local tropical cyclone frequency and intensity in combination with population exposure demonstrates that Harris County is at high risk for hurricane hazards. SLOSH model simulations of Category 5 hurricane storm surges show that under present day sea-level, a significant portion of Harris County is at risk of storm

surge flooding. When combined with sea-level rise, magnitude and extent of flooding are amplified. Exposure of population, highway infrastructure and critical structures and facilities is investigated. Modeling of hurricane storm tide with projected sea-level rise scenarios shows that Harris County is extremely vulnerable to flooding under changing climate. The results suggest that a greater amount of this region's infrastructure is projected to be exposed to damage from hurricane storm surge under sea-level rise scenarios. An expected increase in the frequency of intense hurricanes and sea-levels further exacerbates the vulnerability of this region. Under RCP 8.5, anthropogenic induced climate change is likely to substantially increase the vulnerability of people and infrastructure in greater Houston area to storm surge flooding by 2100.

CHAPTER 1

INTRODUCTION

Coastal regions are characterized by complex interaction of ocean, land, and atmosphere (Kehew 2006). Associated hazards vary from coastal erosion to complete destruction of the coastal regions that became highly developed in the 20th century (Smith 2011). As coastal populations and economies grow in a changing climate, so does their exposure to natural forces. Consequently, coastal environments are becoming higher risk zones and the potential disturbance inflicted on local communities, ecosystems, and economies is a subject of great concern.

According to United States Census Bureau 2016 data, in the United States alone, 94 million people live in coastal counties. This includes areas directly adjacent to the Pacific and Atlantic Oceans as well as the Gulf of Mexico. The Gulf of Mexico and the Atlantic coast regions account for 59.6 million of the entire United States coastal counties population. The population of coastline counties in the Gulf of Mexico region increased by more than 3 million people, or 24.5 percent between 2000 and 2016, the fastest growth among coastline regions. By comparison, the entire United States grew by 14.8% over the same period (U.S Census Bureau 2018). This is important because in North America, the Gulf Coast region is one of the primary targets for tropical storms and hurricanes, and the hazards related to them affect the regional gross domestic product (GDP) and cause injuries, fatalities, and associated psychological stresses (Emanuel 2011).

Motivation

In order to minimize the disruption of coastal communities by tropical cyclones it is of importance to study their complex behavior. Tropical storms can be formed by disturbances in the Trade winds, tropical waves, thunderstorm activity, low shear of horizontal winds, and sea surface temperature above 26.5°C. Dynamic and statistical weather models have successfully predicted the track and strength of hurricanes within the time scale of weather forecasting; however, uncertainties remain due to model resolution, parameters and the lack of data.

While damage from a hurricane may be caused by wind, rain-induced flooding, and mudslides, history shows that storm tides have resulted in the most devastation and greatest number of fatalities (Fitzpatrick 2014). Storm surge being one of the most dangerous natural hazards, it is important to examine the effect of sea-level rise on storm surge induced flooding. The effects of potential sea-level rise on the communities in the Gulf Coast region need to be considered. The combined influence of increase in weather extremes and sea level rise will thus likely impact the local communities in the future.

Objectives

The main purpose of this study is to perform a geospatial analysis of hurricane flood hazard zones caused by storm-tides along the Texas coast. Overall, this study's objectives are to construct spatial models of local tropical cyclone frequency and intensity and evaluate the impact of sea-level rise and storm surges on local

communities by combining a range of sea-level rise scenarios with the potential maximum storm surge levels.

Study Area

The statement by Stephen Wheeler and Timothy Beatley (2014) that cities today are on the front lines of climate change cannot be overemphasized. Multiple stresses on urban environments introduced by climate change and global warming have already been identified and are projected to get worse unless strong mitigation and adaption plans are implemented. Due to dense population and development, economic activity and infrastructure, cities are also the most vulnerable entities to direct and indirect effects of climate change. Urbanization increased in the Texas coastal communities, particularly in the Houston metropolitan area during the recent decades (Figure 1-1). Based on the last United States Census Bureau data, Houston experienced tremendous growth. For instance, population of Harris County grew from 3,400,578 to 4,092,459 from 2000 to 2010 which is equivalent to 20.4% increase. Population of nearby Galveston and Chambers counties increased by 16.4% and 34.8% respectively. As can be seen in Figure 1-1, although net population change in these counties is positive, some communities experienced population decline. Those that did have an increase in population, however, saw a significant change. For example, the community of Beach City saw a tremendous growth of 95.4%, South Houston 68.4%, and League City 153.3% for one of its Census tracts. These trends are critical because in North America, the Gulf of Mexico is one of the primary targets for tropical storms and hurricanes. Although any geographic location along the Gulf Coast is at risk for hurricane-induced

storm tides, taking into consideration a classical definition of risk being a product of hazard, exposure of people and structures, and vulnerability of population and structures, it becomes obvious that certain areas of the State of Texas are at higher risk than others. Metropolises such as the city of Houston and its neighboring communities are growing along and near coasts which makes them especially vulnerable to some of the costliest hazards such as hurricane force winds and flooding. Furthermore, climate change increases the vulnerability of these regions. Increases in large storm tides and sea level in a changing climate have potentially the most damaging impacts to these communities and their economies and infrastructure.

For this study, the coast of the State of Texas with focus on the Houston metropolitan area including Harris County, the largest and most populated county in southeastern Texas, was chosen to analyze flood risk from hurricanes, storm tides and future climate change-induced sea-level change. This coastal low-lying land is adjacent to a wide and flat continental shelf of the Gulf of Mexico that makes it extremely vulnerable to storm tides.

Historically, many hurricanes made landfall in and near Southeastern Texas, some of which resulted in catastrophic destruction of life and property. Tracks of major historical hurricanes that came ashore the Texas coast are shown in the Figure 1-2. The Galveston Hurricane of 1900 was the most devastating hurricane in recorded history in terms of loss of life and property (Keim and Muller 2009). A more recent example is Hurricane Harvey, that made landfall near Rockport, Texas generated record-breaking flooding, mostly by heavy precipitation, in the Houston metropolitan area, in particular in Harris County.

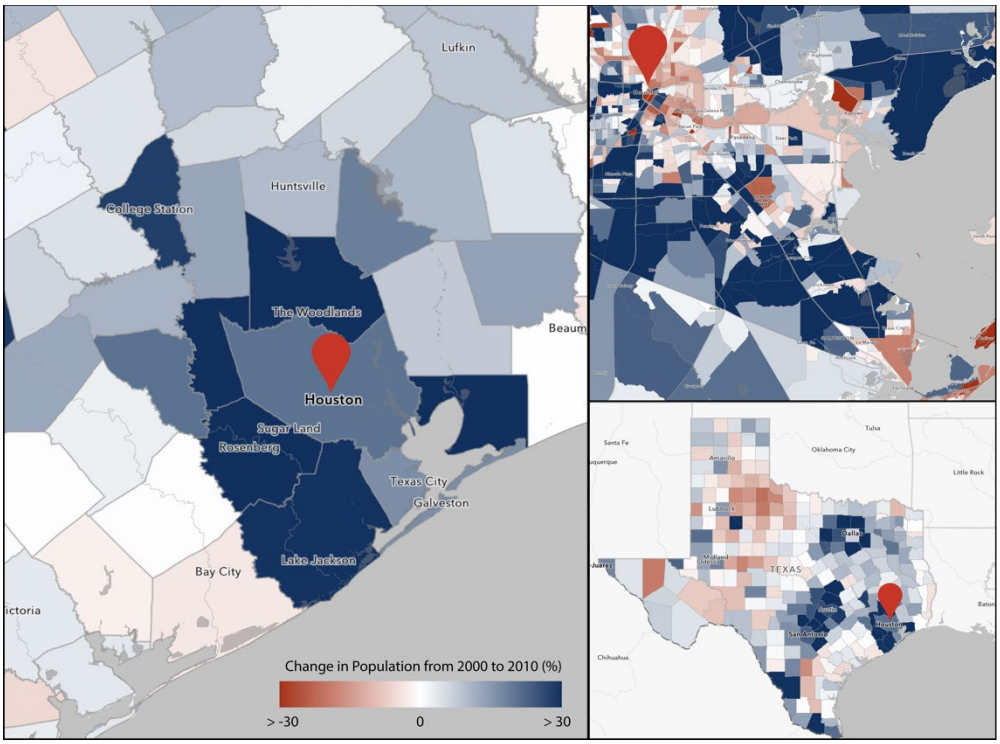

Figure 1-1 Change in population in the Houston metropolitan area from 2000 to 2010.

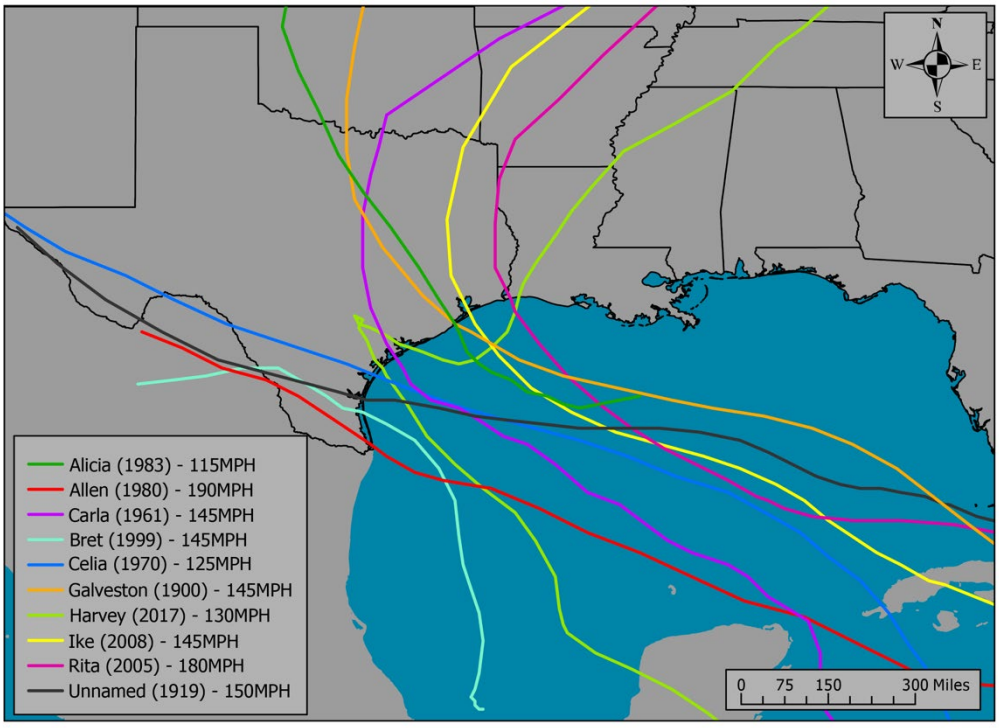

Figure 1-2 Major historical hurricane tracks. Data obtained from NOAA's Atlantic Oceanographic and Meteorological Laboratory (https://www.aoml.noaa.gov).

Climatology of Tropical Cyclones on the Texas Coast

Historical data of tropical storms and hurricanes are of importance for the Texas coast. It provides better understanding of their frequency and magnitude. Climate change will likely produce stronger hurricanes in the future, thus further increases the need to analyze the regional hurricane climatology. In this section, tropical cyclone data from 1851 to 2018 are examined. In the following, hurricane climatology for the entire Atlantic basin, Gulf of Mexico, and contiguous United States are also discussed.

Many tropical cyclones originated in the North Atlantic over the span of 168 years of available historical data. The most recent reanalysis of revised Atlantic hurricane database (HURDAT2) contains 1874 tropical cyclone records of variable strength and characteristics. As can be seen in the Figure 1-3, tropical storms form in the region of North Atlantic between 5 – 25 degrees north. Due to their cyclonic nature, tropical cyclone cannot form below 5 degrees north due to negligible Coriolis force (Wallace and Hobbs 2011). Tracks of these storms, descriptive statistics of annual occurrence rate, as well as distribution of storms classified by Saffir-Simpson scale (Figure 1-3). The frequency of tropical cyclones in the Atlantic basin is approximately 11 every year. Maximum number of storms recorded in this time period is 30 in 2005. Minimum is 1 in 1914. Standard deviation of the dataset is 5.6. From the entire record, 13% never reached a strength of a tropical storm. 37% were classified as tropical storms with the winds ranging from 39 to 73 miles per hour, 32% had hurricane strength winds of 74 to 110 miles per hour, and 18% reached the wind speeds greater than 110 miles per hour during their lifetime. This distribution reveals that the majority of the tropical storms forming in the tropical Atlantic Ocean increase in strength to hurricanes Category 1 or

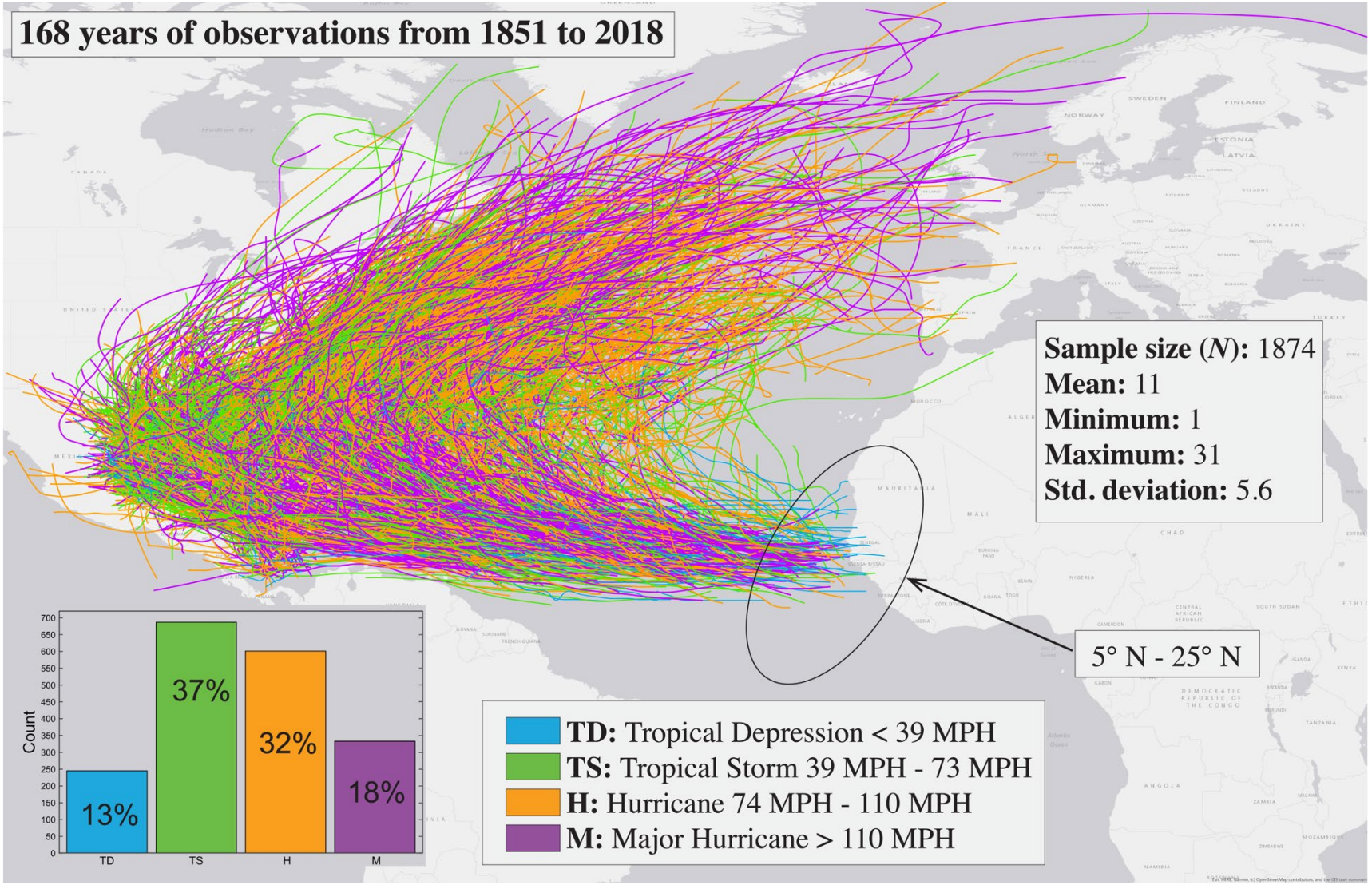

Figure 1-3 Atlantic Basin hurricane tracks from 1851 to 2018 (Data source: National Hurricane Center).

higher.

A subset of the HURDAT2 dataset for the storms that made landfall on 367 mile stretch of the State of Texas is presented in the Figure 1-4. Analysis of hurricane tracks demonstrates that most common heading direction is south east (Figure 1-5). After making landfall, storm tracks appear to follow three main patterns that are related to prevailing weather patterns. Storms that hit northern and central portion of the state tend to curve north or north east going through the eastern and central regions of the state. Storms such as Celia (1970), Bret (1999) and Allen (1980) (see Figure 1-1) that strike in the south, tend to stay on more westward path. Distribution of storms by strength is similar to those of the entire Atlantic basin.

In Figure 1-6 tropical storm and hurricane counts for the Atlantic basin, contiguous United States, Gulf of Mexico and the State of Texas were aggregated by decade from 1850's to 2010's. Table 1 represents the same data for four regions but as a heat table. 2000's was the decade with the most tropical cyclones across all basins except Texas. The period from 1940 to 1950 was the most active decade in terms of the total number of tropical cyclones. However, while most hurricanes and total number of cyclones occurred in this period, the period from 2000 to 2010 encompassed the most numbers of cyclones. Additionally, linear models were applied to tropical storms, hurricanes and to the sum of both to demonstrate any possible trends. Linear fitting for tropical storms is shown in black, hurricanes blue and the sum of both in red. Figure 1-6 displays an increasing trend for all tropical cyclones and tropical storms across four basins from 1850 's to 2010's. The upward slope of the trend of tropical cyclones in the Atlantic basin is most pronounced while the slope is less inclined for the Texas coast.

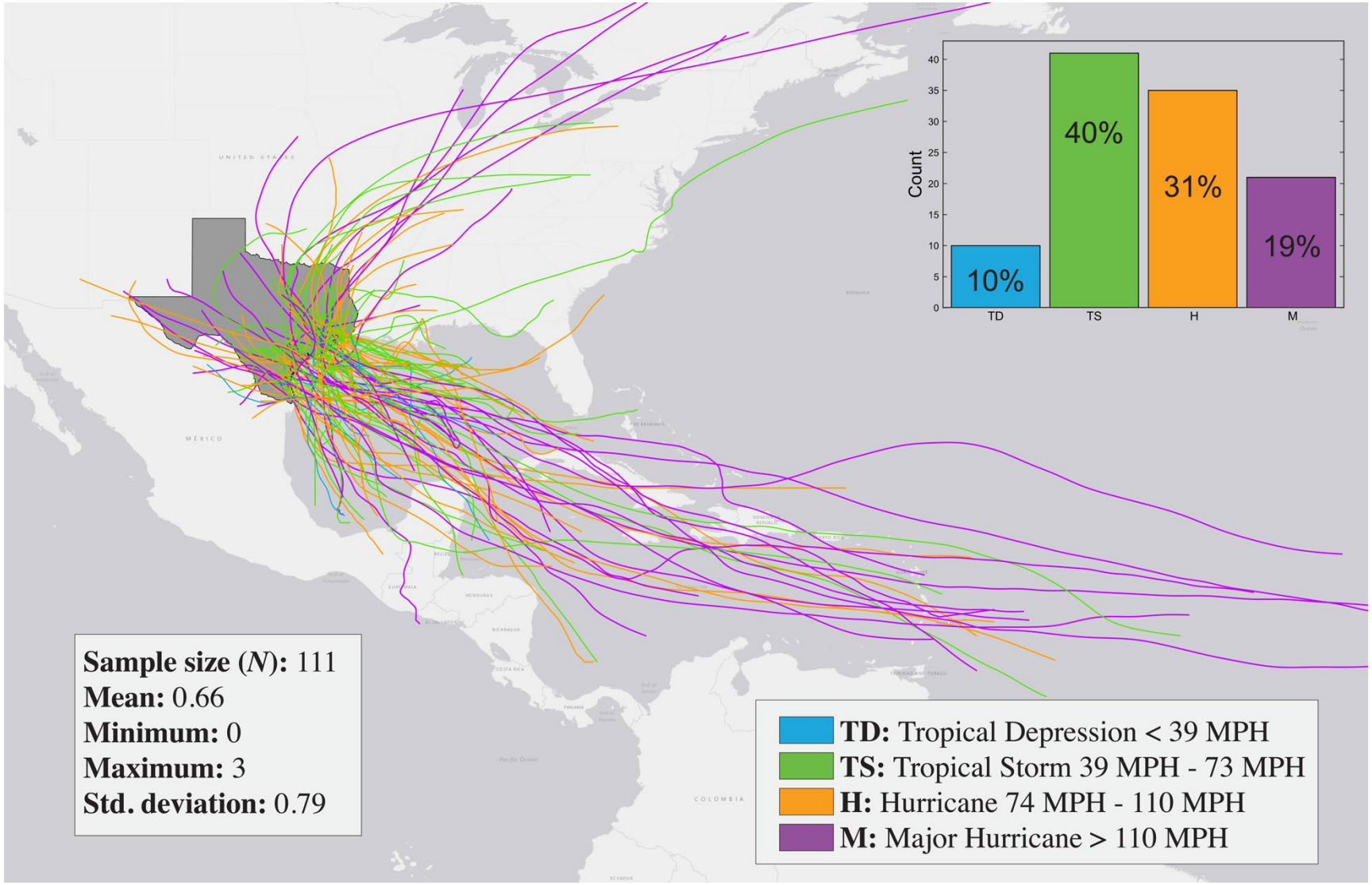

Figure 1-4 Texas landfalling hurricanes from 1851 to 2018 (Data source: National Hurricane Center).

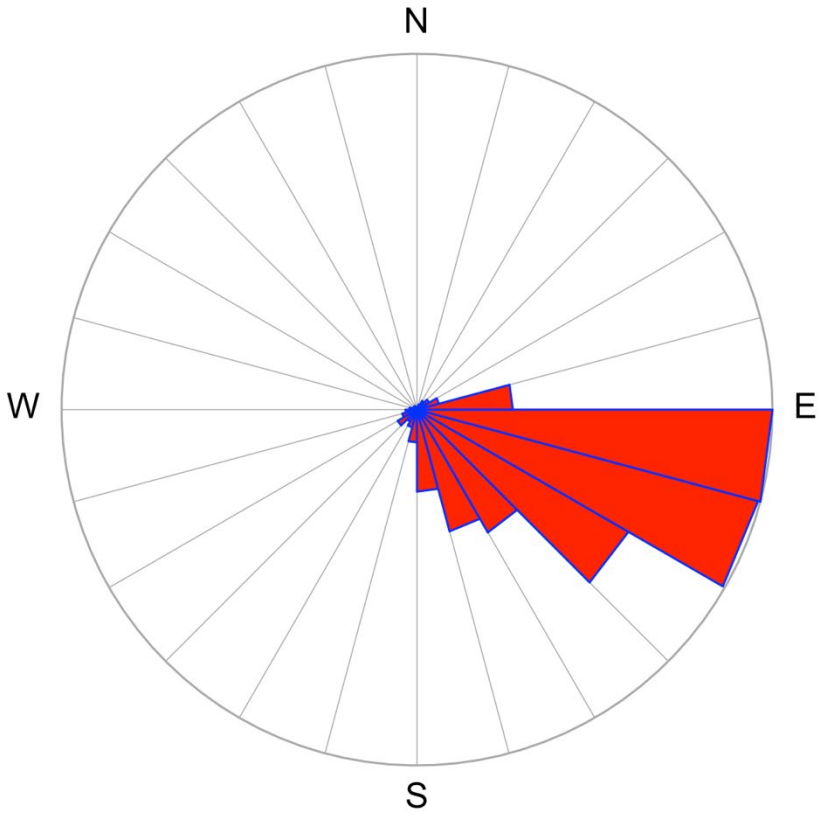

Figure 1-5 Heading of hurricanes approaching the coast of Texas.

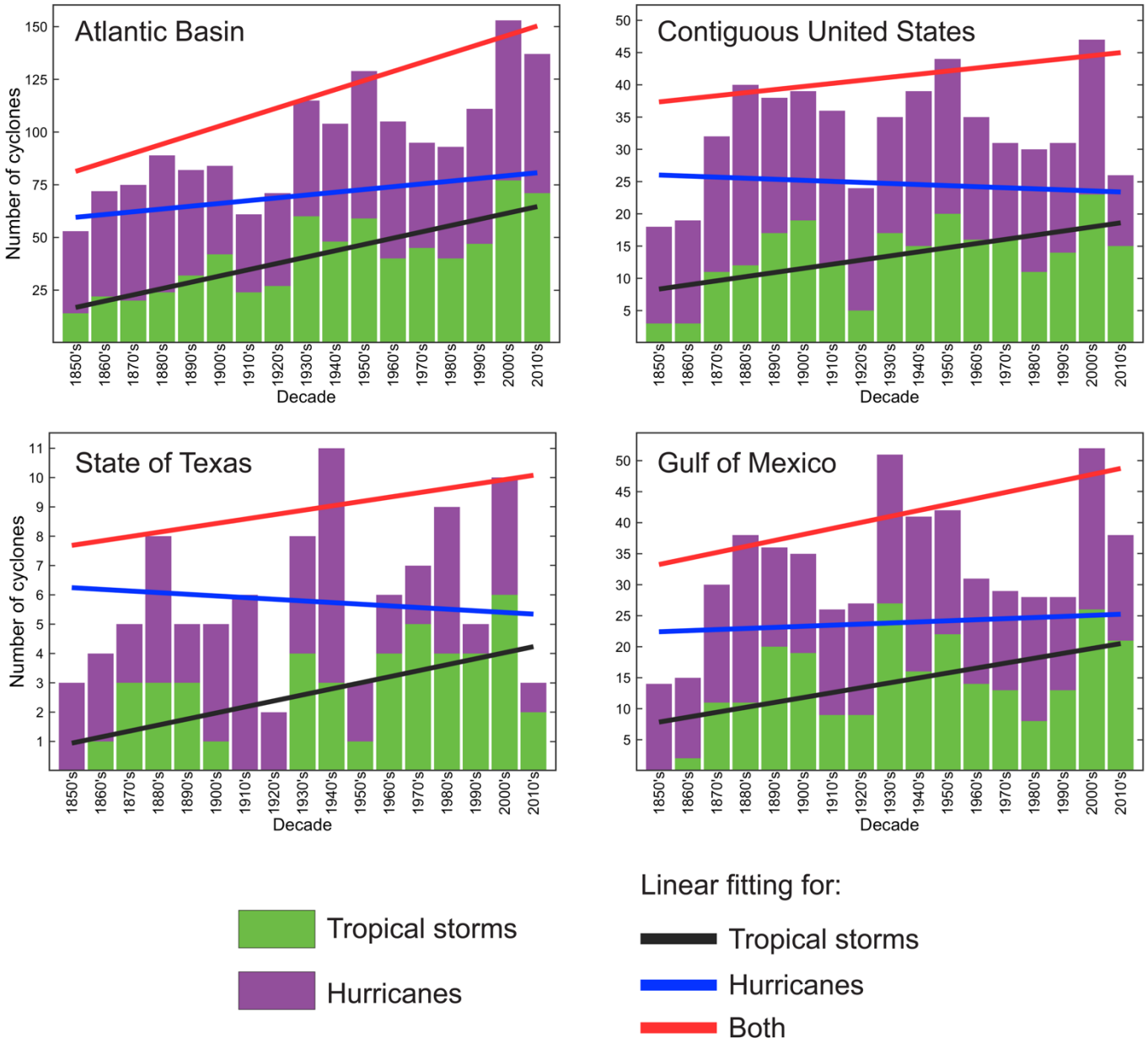

Figure 1-6 Counts of Atlantic hurricanes for four basins aggregated by decade (data from National Hurricane Center).

Table 1 Tropical cyclone counts aggregated by decade (data from National Hurricane Center)

	Atlantic Basin			United States			Gulf of Mexico			Texas		
Decade	Tropical storms	Hurricanes	Both	Tropical storms	Hurricanes	Both	Tropical storms	Hurricanes	Both	Tropical storms	Hurricanes	Both
1850's	14	39	53	3	15	18	0	14	14	0	3	3
1860's	22	50	72	3	16	19	2	13	15	1	3	4
1870's	20	55	75	11	21	32	11	19	30	3	2	5
1880's	24	65	89	12	28	40	11	27	38	3	5	8
1890's	32	50	82	17	21	38	20	16	36	3	2	5
1900's	42	42	84	19	20	39	19	16	35	1	4	5
1910's	24	37	61	12	24	36	9	17	26	0	6	6
1920's	27	44	71	5	19	24	9	18	27	0	2	2
1930's	60	55	115	17	18	35	27	24	51	4	4	8
1940's	48	56	104	15	24	39	16	25	41	3	8	11
1950's	59	70	129	20	24	44	22	20	42	1	2	3
1960's	40	65	105	16	19	35	14	17	31	4	2	6
1970's	45	50	95	16	15	31	13	16	29	5	2	7
1980's	40	53	93	11	19	30	8	20	28	4	5	9
1990's	47	64	111	14	17	31	13	15	28	4	1	5
2000's	77	76	153	23	24	47	26	26	52	6	4	10
2010's	71	66	137	15	11	26	21	17	38	2	1	3
Total	**692**	**937**	**1629**	**229**	**335**	**564**	**241**	**320**	**561**	**44**	**56**	**100**
Annual average	**4.1**	**5.6**	**9.7**	**1.4**	**2**	**3.4**	**1.4**	**1.9**	**3.3**	**0.3**	**0.3**	**0.6**

Figure 1-7 displays an increasing trend of hurricanes Category 3 and higher across four basins from 1850's to 2010's. The increasing rate of major hurricanes overtime is only found to be statistically significant for the Atlantic Basin ($r^2 = 0.616$, p-value < 0.001). For the other three basins the linear model explains less than 14% of the variance in number of hurricanes. Observed upward trend for hurricane events has been attributed to the current change in climate and is addressed in the next section. The increasing rates of tropical storms, however, have been linked to limited historical data.

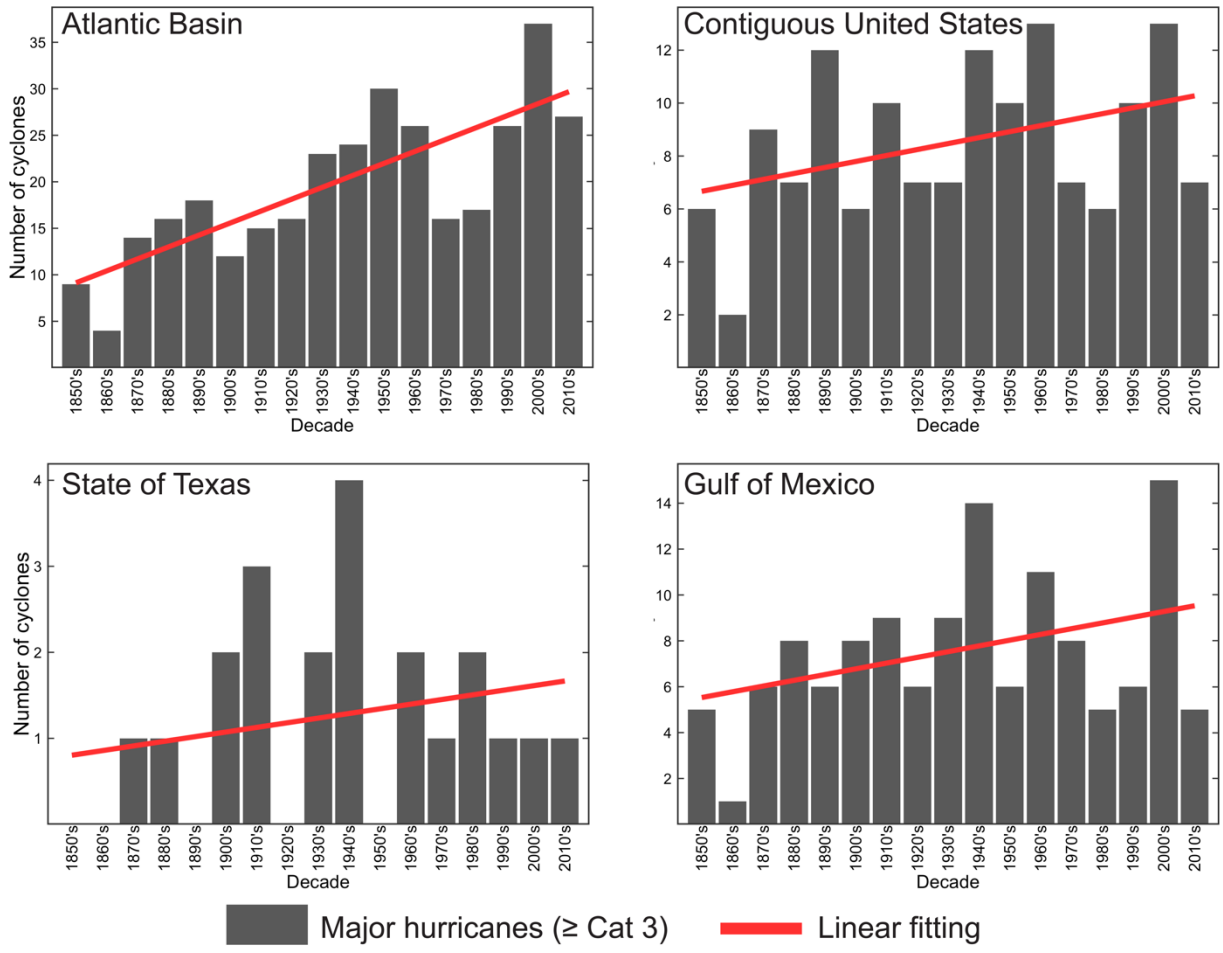

Figure 1-7 Counts of major historical hurricanes aggregated by decade.

Hurricanes and Climate

Increasing tropical cyclone rates, destructiveness, and geographic locations they affect have been under discussion due to change in the climate. Tropical cyclone intensity could increase with warming of the sea surface. A great number of observational and numerical modelling studies have been carried out to address this important question (Yoshimura and Sugi 2005; Held and Zhao 2011; Sugi et al. 2012; Zhao et al. 2013; Walsh et al. 2015). Both types of studies have found that anthropogenic climate change and global warming has contributed to an increased tropical cyclone intensity and the rates of intense hurricanes (Kossin et al. 2017). Anthropogenic induced climate change is likely to increase high intensity events and diminish global frequency of lesser storms (Emanual 2011). In addition to Coriolis force and vertical shear of horizontal winds, tropical storm formation and life cycle are highly dependent on sea surface temperature for heat and moisture that fuel their circulation (Mctaggart-Cowan et al. 2015). It has been shown that global average sea surface temperatures (SST) have certainly increased since the 1950's. From 1950 to 2009 average SST risen 0.41 ^{o}C in the Atlantic, 0.65 ^{o}C in the Indian and 0.31^{o}C in the Pacific Ocean (IPCC 2013). Even small changes in sea surface temperature increases the thermodynamic potential for hurricanes and therefore lead to more destructive storm events (Emanual 1987). These findings agree with Elsner et al., who found a 30-year trend of Atlantic tropical cyclone intensification due to warming ocean temperatures (Elsner et al. 2008). As discussed above, negative trend in hurricane frequencies for the United States and Texas derived from HURDAT2 dataset can be explained by recent

numerical and statistical simulations that project a poleward shift of the tropical cyclone tracks (Bloemendaal et al. 2020).

Increased rainfall by incline in the tropical storm intensity will likely result in severe flooding. Knutson et al. (2019) demonstrate that there is at least medium to high confidence that a 2 ^{o}C global warming will increase global tropical cyclone precipitation rates. Another major effect of climate change on tropical storm activity is sea level rise. According to Knutson et al. (2019), the most confident change in impacts of tropical cyclones is the higher storm surge inundation due to global warming induced sea level rise. With all of this in mind, hurricane flood hazards become a great concern. In further chapters we explore the effect of higher sea level on storm surge inundation and assess the potential impacts of storm surge under these conditions.

CHAPTER 2

HURRICANE FLOOD HAZARDS

Introduction

In this chapter, we present a spatial approach for assessing hurricane flood hazards. The first section of this chapter documents data used in this study. The second section describes the development of spatial models for hurricane hazards analysis.

Observations for tropical cyclones have been gathered from historical and instrumental records such as satellites, radar, weather buoys, and aircrafts. Historical observations were reported when tropical cyclones were directly encountered by ships or when they made landfall in populated places (Keim and Muller 2009). First reconnaissance aircraft mission was accomplished by Joseph P. Duckworth and Ralph O'Hair on July 27, 1943. Since then hurricane reconnaissance by aircraft has become routine, and today it is one of the most important tools for determining hurricane position and characteristics. However, the most important technological advance in storm monitoring and forecasting did not occur until 1966. This is because it was not until 1966 that the first completely operational weather satellite was launched into orbit. This satellite orbited over the poles at low altitude and took pictures of the Atlantic basin once a day (Elsner and Kara 1999). Remote sensing data and more sophisticated aircraft and marine instruments improved the reliability of the tropical cyclone records since the 1970s. Other advances in tropical storm forecasting included the use of ocean data buoys starting in 1970's and deployment of Doppler radar in the 1990's. Needless to say, the spatial density and accuracy of tropical cyclone observations is steadily

increasing today due to technological innovations and the need for more accurate hurricane forecasting.

Several meteorological organizations around the world record raw tropical cyclone data which is then carefully analyzed by meteorologists to produce “best-track” data. Tropical cyclone data used in this chapter came from several sources described below.

In the United States, the storm track data for every six hours is collected and reported by the National Hurricane Center (NHC), a division of National Oceanic and Atmospheric Administration (NOAA). After the storm moves out of the forecast area or dissipates, the NHC conducts a post storm reanalysis of each tropical storm and produces the “best-track” data. In 2000, NHC began a program called Atlantic Hurricane Database Re-analysis Project with the goal of extending the database from 1871 back to 1851 and revising it using newly available meteorological and historical data, methods and technologies. Most recently, this includes the reanalysis of 1961 – 1965 hurricane season (Delgado and Landsea 2018). Most characteristics of tropical cyclones that were used as variables in this study came directly or were derived from NHC’s revised Atlantic hurricane database version 2 (HURDAT2) (Landsea and Franklin 2013). Data for the radius, heading, and forward velocity is not available through HURDAT2 “best-track” database. Hurricane heading and forward velocity can be derived from HURDAT2 by using the storm’s position and time. For the radius of maximum winds other sources should examined. In 2013 National Center for Atmospheric Research’s (NCAR) Research Applications Laboratory (RAL) began its own Tropical Cyclone Data Project (TCDP) with the goal of providing high quality

database that includes several hurricane wind parameters. The third phase of this project was comprised of constructing a dataset of tropical cyclone size and radial structure utilizing data from the QuickSCAT satellite. The final phase of the TCDP was comprised of using the Enhanced Vortex Data Messages (VDM+) and Flight Level (FLIGHT+) datasets to build a new historical Tropical Cyclone Observations-Based (TC-OBS) database (Vigh et al. 2016).TC-OBS database includes observation-based estimates of radius of maximum wind (RMW) that can used for the development of spatial distribution models. RMW of storms not included in TC-OBS can be obtained from International Best Track Archive for Climate Stewardship (IBTrACS) dataset (Knapp et al. 2018).

Time period of available tropical cyclone data is important. The HURDAT2 re-analysis database extends back to 1851 and TC-OBS to 1989. However, the majority of the older storms are missing observations for central pressure and radius of maximum winds (RMW). Additionally, statistical uncertainty of storms' parameters is higher for older events recorded before instrumental measurements became routine.

Methods

This section presents the development of spatial distribution models for assessing hurricane hazards on the Texas coast using tropical cyclone track data. Exposure and vulnerability of population and the concerns of climate change impacts on these variables were discussed in Chapter 1. Therefore, this section focuses on tropical cyclone hazards. Severity is described in terms of cyclone intensity and likelihood in terms of frequency. Spatial models illustrated here were created by utilizing spatial grids

framework developed by Elsner et al. (2012) for hurricane climate research. This method involves hexagon tessellation of the basin and populating the resulting grid with local cyclone tracks and attributes.

Before a spatial grid can be constructed and distributed with tropical storm parameters, raw hurricane data need to be analyzed and processed. TC-OBS data has cyclone observations 1 hour apart, while IBTrACS track data is 3 hours apart. HURDAT2 “best-track” data consists of cyclone observations in 6-hour intervals. These inconsistencies present a challenge for integrating the three datasets into one, and in addition, in their raw format HURDAT2 and IBTrACS track data are not resolved enough for spatial analysis and modeling. In order to address this challenge a piecewise polynomial function was used to interpolate the track observations to 1 hour (Jagger and Elsner 2006). This way the three datasets can easily be integrated to provide high resolution attributes for hurricane tracks. After integration is complete, hurricane attributes can be aggregated for each grid cell. For hazards analysis, maximum wind speed and number of observed cyclones are obtained within each hexagon. The assumption here is that the maximum wind speed within the hexagons will likely depend on the number of cyclones that crossed that region. This hypothesis can be tested by computing Pearson’s product-momentum correlation coefficient for the two variables. The result reveals that there is a significant positive association ($r = 0.8$). More importantly, using this information we can now construct a composite score of the two variables representing an average degree of hurricane hazards for local coastal areas.

Results

The results of this assessment are presented in the Figures 2-1 to 2-3. Local tropical storm frequency for 1851 – 2018 time period is demonstrated in the Figure 2-1. Each grid has 12,720 hexagons across the entire domain. As can be seen, the highest frequency occurs in the Central North Atlantic, although high concentration areas are also recorded in the Gulf of Mexico, particularly of the coast of Louisiana, and in Yucatan Basin. Tessellation of highest intensity reveals a slightly different pattern (Figure 2-2). It is observed that the most severe hurricane winds have been recorded off the west coast of Mexico, the State of Florida and over the Bahamas.

One of the objectives of this study being the geospatial analysis of hurricane flood hazard zones caused by storm-tides along the Texas coast, we now turn our attention to the State of Texas. Figure 2-3 shows the composite score of local maximum hurricane intensity and frequency on the scale from 1 to 5. Localities with the score of one being at the very low risk for hurricane hazards and with the score of 5 at the very high risk. As discussed previously, because the State of Texas historically has been the region where hurricanes crossed, the entire stretch of its coast is at risk. However, as can be seen in the Figure 2-3, Cameron County in South Texas and Brazoria County in Southeast Texas are at a very high risk. These regions are at the highest risk for hurricane hazards under consideration of development, and population growth and density. Thus, the Houston metropolitan area in Harris County is a highly suitable example for hurricane flood hazards analysis.

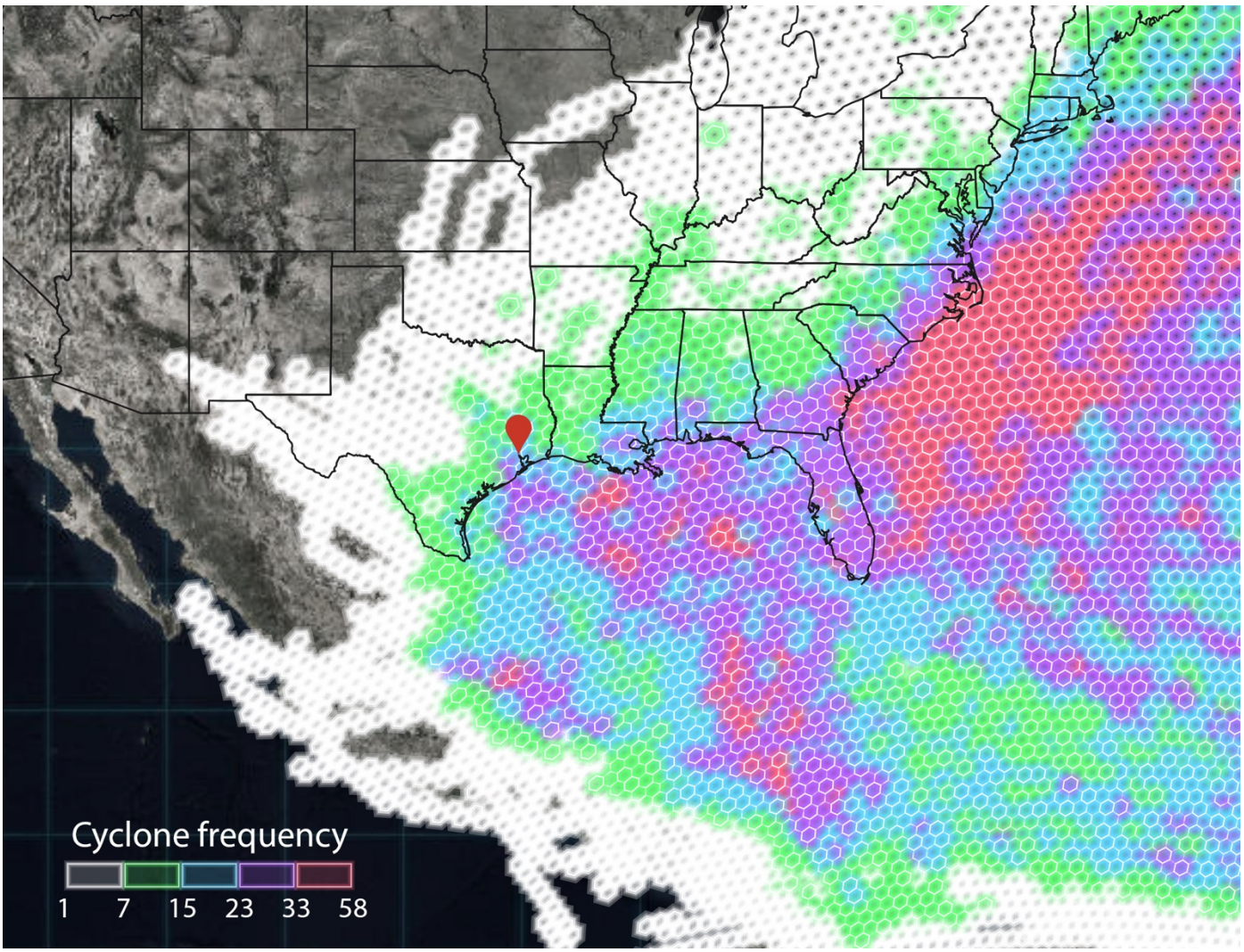

Figure 2-1 Local frequency of cyclones for 1851- 2018 time period (constructed by using HURDAT2 and IBTrACS track data).

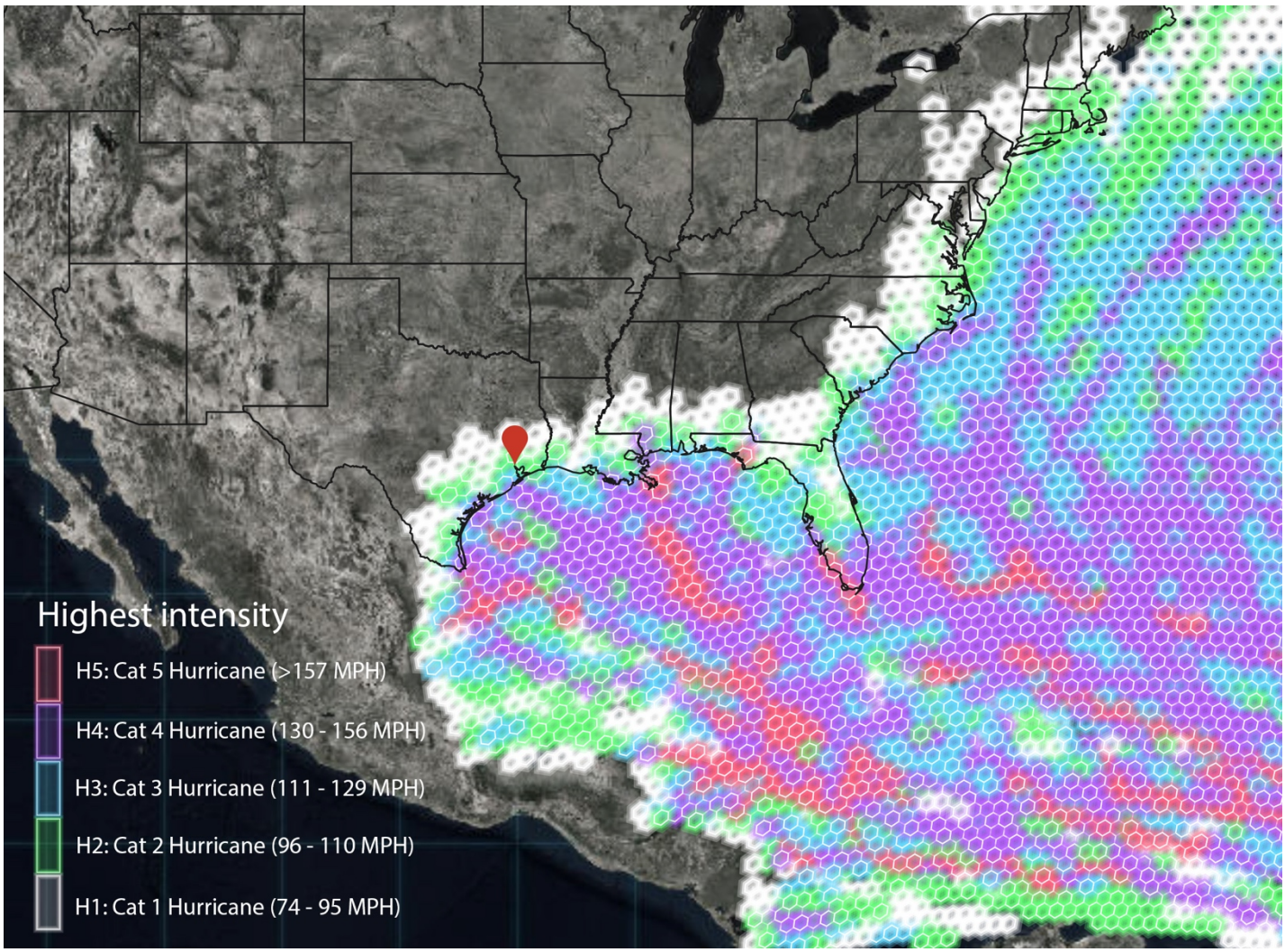

Figure 2-2 Local maximum intensity of hurricane winds (constructed by using HURDAT2 and IBTrACS track data).

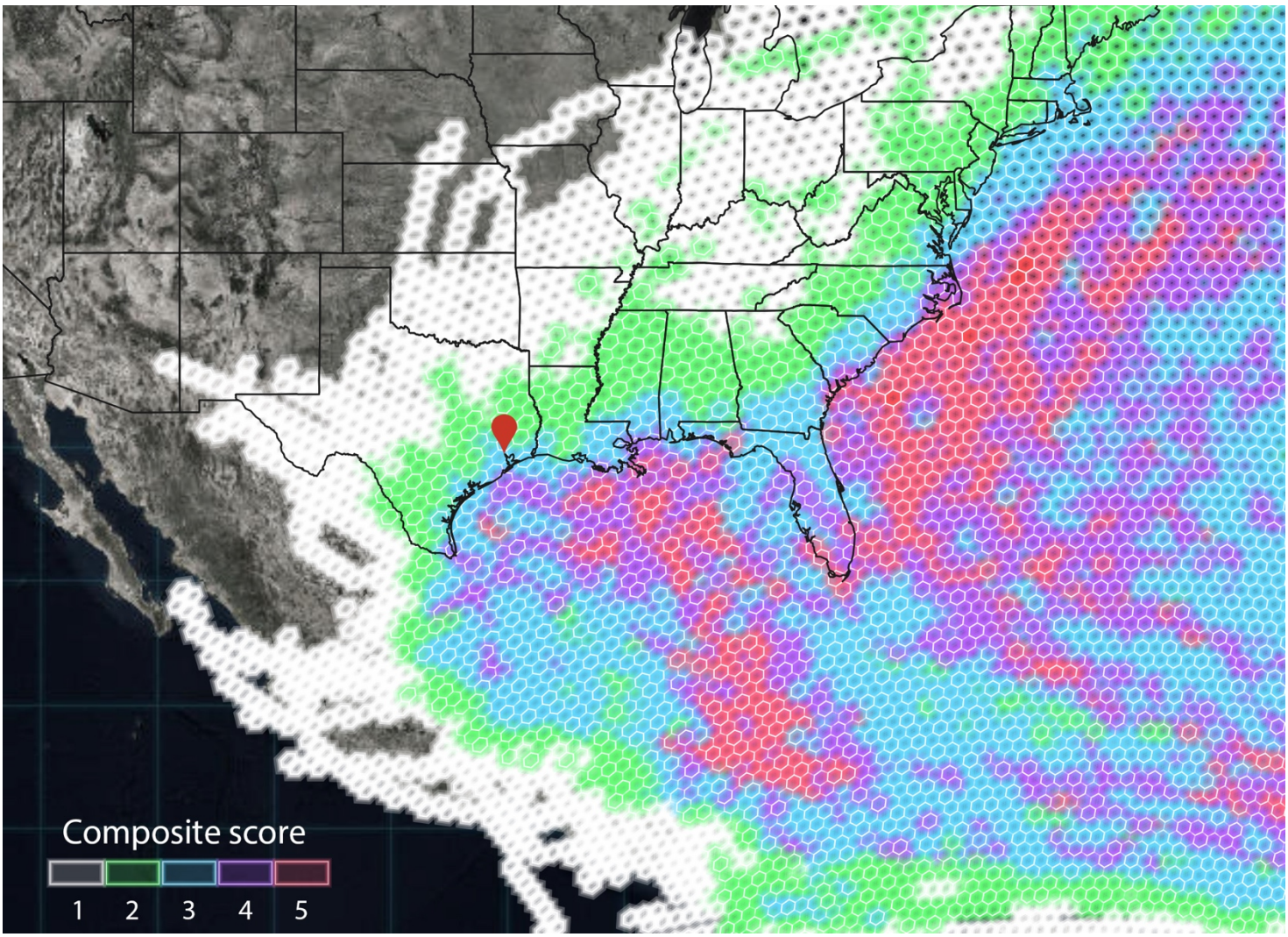

Figure 2-3 Average local risk of hurricane hazards (estimated by using HURDAT2 and IBTrACS tropical cyclone data).

CHAPTER 3

SEA-LEVEL CHANGE

Introduction

Sea-level is affected by multiple physical processes with different temporal scales (Figure 3-1). On shorter time scales, sea-level changes due to solar, lunar and other planetary tides, wind and internal waves, swell, and storm surges and tides. On longer time scales, the sea level elevation is affected by changes in ocean currents (also referred as dynamic sea level change), calving of glacier and ice shelves, river discharge, thermal expansion or contraction, atmospheric pressure change, salinity contraction or expansion, and wind stress. On geologic time scales, sea-level varies due to tectonic, glacial, sedimentary and eustatic processes (Dolan and Lins 1985). In addition, sea-level is not uniform throughout the continents, and therefore regional and local variations also exist.

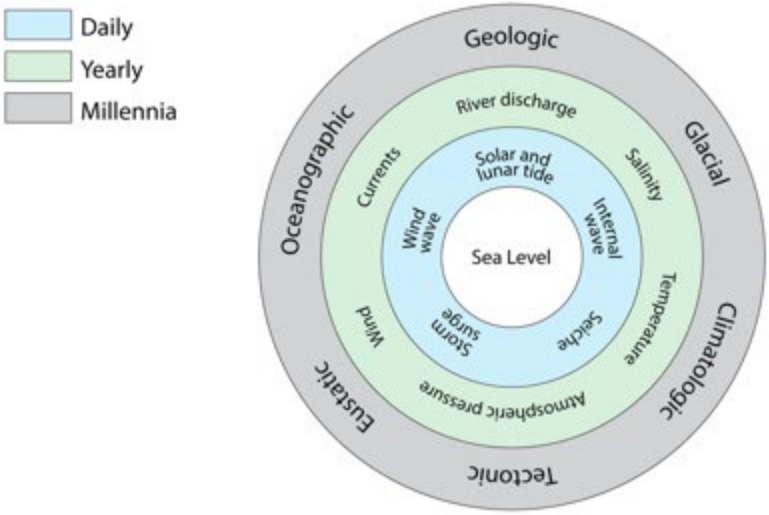

Figure 3-1 Cumulative sea-level variations over a wide range of time intervals (modified from Dolan and Lins 1985).

In all, there are two factors that contribute to regional change in sea-level (Figure 3-1). The first factor is the global change in sea level that is referred to as eustatic sea level change. Change by tectonic processes (e.g. change in ocean volume by plate tectonics) and climatic process (e.g. melting of glacier, ice sheets, and thermal expansion or contraction). The second factor in addition to the global change considers local tectonic processes and vertical displacement of land by riverine sediment deposits, coastal erosion, and local man-made disturbances by exploration of natural resources and is referred to as relative sea level (Klein and Nicholls 1998). This chapter mostly focuses on sea-level change confined to the study area.

Thermal (steric) expansion and melting of ice sheets and glaciers due to current episode of global warming have been the main contributors to global sea-level rise. In the recent decades the planet has been adjusting to increasing greenhouse gases (GHG) released to the atmosphere by storing the resultant heat in the oceans. Water from melting glaciers and ice sheets as well as thermal expansion have been demonstrated to raise sea levels through the increase of ocean volume. Figure 3-2 shows reconstructed global average sea-level from 1880 to 2013 (Church and White 2011). Satellite altimeter data from TOPEX/Poseidon is shown in red (1993 to 2015), and in-situ data from coastal tide gauges since 1880 to 2013 in blue. The most recent satellite data has measured a rise in global mean sea level (GMSL) of 0.12 in/year. This is equivalent to the cumulative sea level rise of 2.8 inches over the last 25 years (Nerem et al. 2018).

According to IPCC Fifth Assessment Report (AR5), regional sea-level is likely to experience a large deviation from the global mean in the 21st century, with some places

having significantly higher rates of sea-level rise (Church et al. 2013). In fact, the sea-level rise rates in Texas have been higher than in most other coastal states in the United States. Sea-level changes in Texas are attributed to global sea-level change (due to melting of ice sheets and glaciers, eustatic rebounds and thermal expansion) and regional sea-level change e.g. linked to land subsidence by compaction of sediments and groundwater extraction. Glacial isostatic adjustment and sediment compaction have been estimated to add 7.9×10^{-3} – 7.9×10^{-2} in/year to relative sea rise in Texas and similar regions (Kopp et al. 2016). Ground water and oil/gas extraction further contribute to cumulative relative sea level rise in this region (Eggleston and Pope 2013).

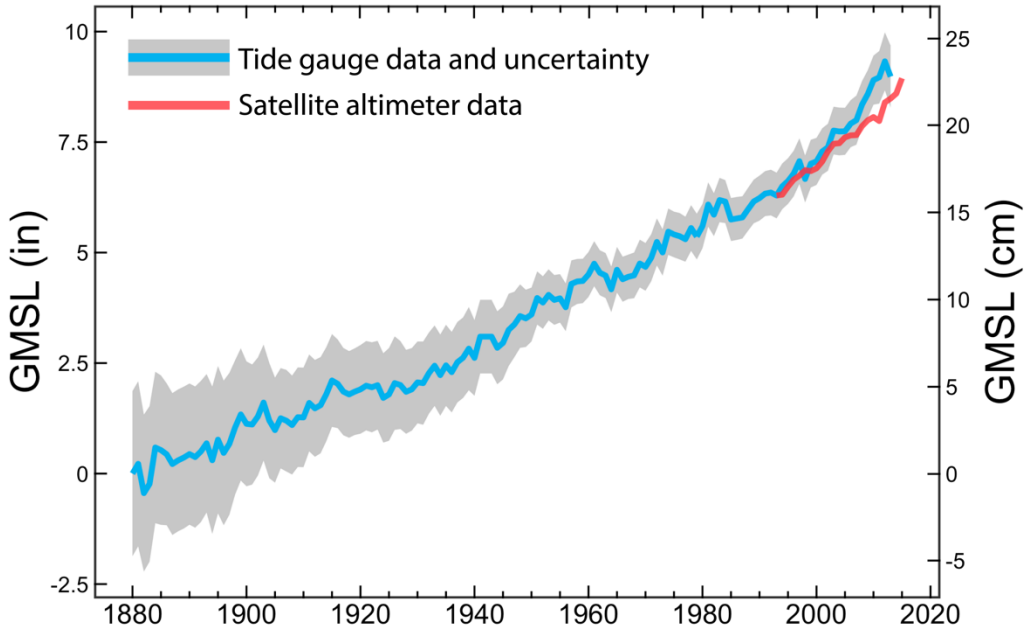

Figure 3-2 Global average sea level from 1800 to 2015 (data from Church and White 2011).

Methods

For the analysis of sea-level trend, verified water levels were obtained from National Oceanic and Atmospheric Administration's (NOAA) Tides and Currents data repository. The sea-level data from four tide gauge stations were used to plot time series.

Representative Concentration Pathways RCPs provide a range of possible future greenhouse and aerosol emissions based on historical trends for the evolution of atmospheric composition (Moss et al. 2010). Representative Concentration Pathway 8.5 (RCP 8.5) scenario is one of the four trajectories into the future based on which we reach 8.5 W m^{-2} radiative forcing from greenhouse gases by 2100, hence its name RCP 8.5. By using statistical and numerical analysis scientists have been able to project future sea-level change using the data from these scenarios.

Based on RCP8.5, the Intergovernmental Panel on Climate Change (IPCC) projects the global sea-level to rise from 3 to 4 ft by 2100 (Church et al. 2013). However, IPCC projection is considered to be on the moderate side, as it does not account for acceleration in the melting of Antarctic and Greenland ice sheets (Zhang et al. 2013). Possible high-end GMSL rise under RCP 8.5 with accelerated ice-melt contributions have been estimated to be between 6 and 8 ft (Jevrejeva et al. 2014; Kopp et al. 2014).

Results

The rates of sea-level rise in Texas have been higher than in most other coastal states in the US and between 0 in and 0.35 in per year (NOAA 2020). Galveston Pier 21

station (number: 8771450) has 105 years of observations and the longest water level record in the Gulf of Mexico. At this location the relative sea-level trend is 0.26 in/year with a 95% confidence interval of +/- $8.7x10^{-3}$ in/year (Figure 3-4a). This is based on monthly mean sea-level data from 1904 to 2018 and is equivalent to a change of 2.14 feet in 100 years. Figure 3-4b shows relative sea-level trend for Galveston Pleasure Pier station (number: 8771510). It is based on tide gauge data from 1957 to 2011. Applied linear model produces the trend of 0.26 in/year with a 95% confidence interval of +/- 0.027 in/year. This is equivalent to a rate of change of 2.17 ft in 100 years. Time series for Corpus Christi (number: 8779770) and Port Isabel (number:8775870) stations are shown in Figure 3-4c and 3-4d. Similarly, long term linear trends demonstrate changes of 1.31 ft per 100 years for Port Isabel and 1.53 ft per 100 years for Corpus Christi.

In addition, sea-level rise enhances coastal erosion by inundation of low-lying coastal regions. A recent study by Nan Xu (2018) found that positive sea-level trend discussed above is partly responsible for the recession of 52.58% of the Texas coast. The results suggest that the region mainly experienced erosion from 1986 to 2015 (r^2 = 0.320, p-value = 0.001). A significant relationship between coastline position and sea-level was observed (r^2 = 0.594, p-value = 0.001). Additionally, a strong association between the rates of sea-level and coastline change was found (r^2 = 0.966, p-value = 0.001).

Under RCP 8.5, historically unprecedented sea-level change is projected by the end of 21st century globally. Therefore, regionalized scenarios are also needed for coastal preparedness and risk management. Sweet et al. (2017) assessed existing global scenarios and developed six local sea-level change scenarios by combining

emissions-dependent probabilistic projections and discrete scenario-based methods. These representative scenarios range from a 1 ft (low-end) to 8 ft (worst case) of sea-level rise, and in addition to GMSL rise drivers, account for vertical land movement and oceanographic processes such as circulation patterns. Four future local relative sea-level scenarios for 2100 (colored lines) and observed annual mean (black line) for Galveston, TX, are shown in Figure 3-3. As it would be expected, due to higher historical rates, climate change related processes and vertical land movement, future sea-level rise projections in this part of Texas are considerably higher than global trajectories under RCP. With the exception of the low scenario, RSL rise in Galveston is projected to be greater than the global average (Sweet et al. 2017).

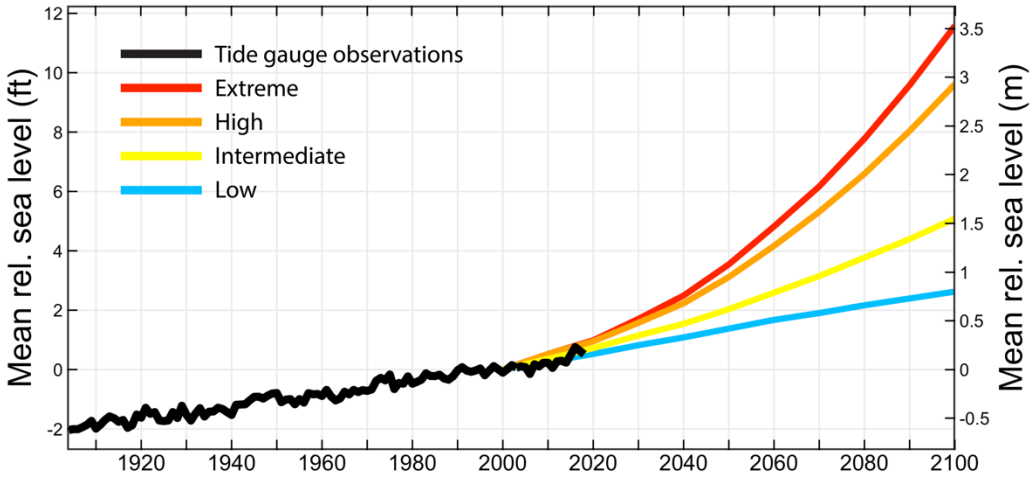

Figure 3-3 Average annual RSL for Galveston, TX with its corresponding (median value) RSL under four scenarios (from Sweet et al. 2017).

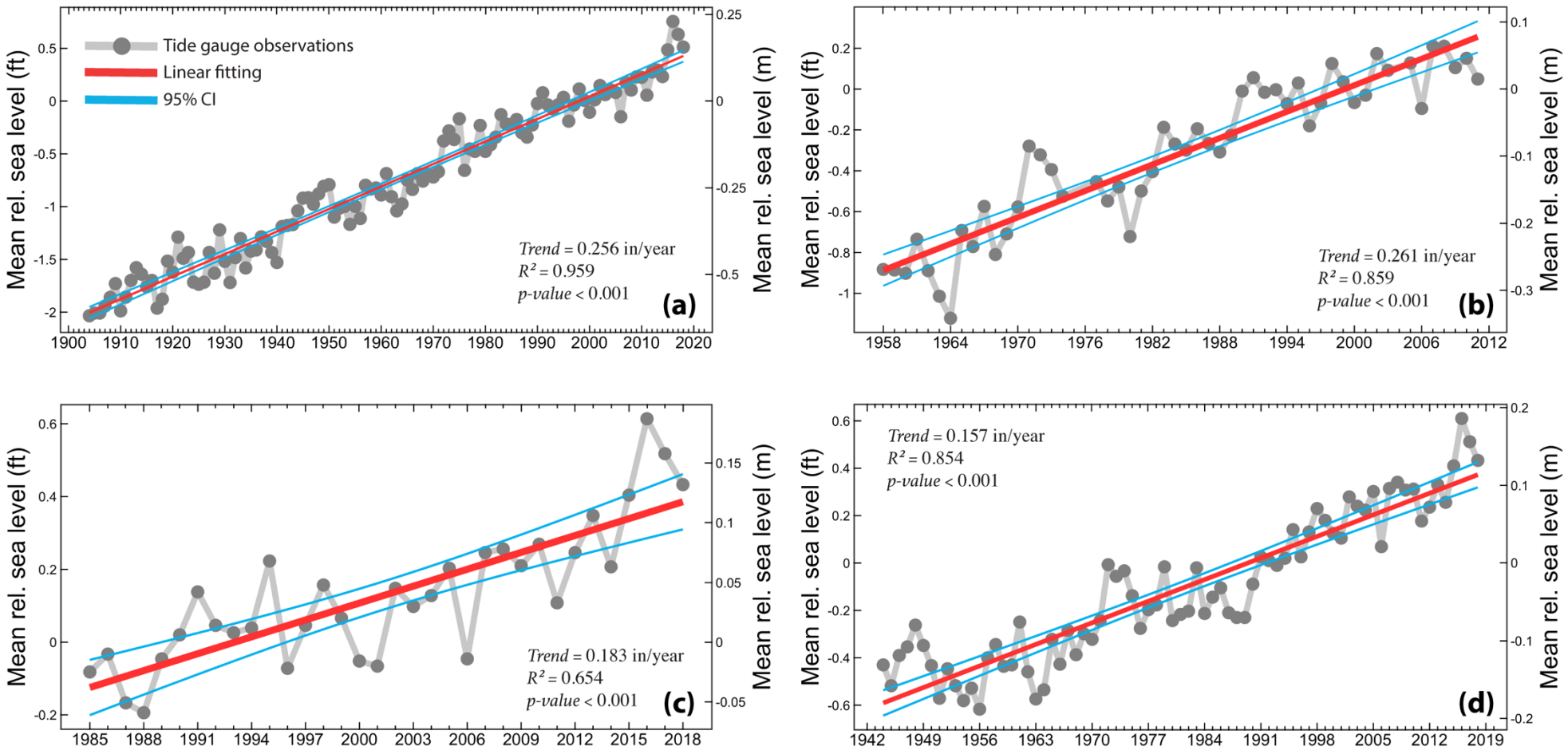

Figure 3-4 Observed annual mean sea-level.

(a) Galveston Pier 21 station. (b) Galveston Pleasure Pier station. (c) Corpus Christi station. (d) Port Isabel station.

CHAPTER 4

STORM TIDE

Introduction

Storm tide is defined as abnormal rise of sea level associated with a tropical or extra tropical cyclone, and it consists of the high tide and the surge induced by a storm (with wind speed larger than 7 on the Beaufort scale or 34 knots). In particular, storm tides are high if the storm surge overlap with the spring high tide.

There are four main components that contribute to a storm surge. These are pressure, wind, wave setups, and geostrophic adjustment. The resultant water-level rise in storm surge depends on the former parameters as well as other global and local factors such as sea-level, tides, bathymetry, and unique topographic characteristics of local peninsula. Perhaps, the most important one in terms of shallow bathymetries such as in the Gulf of Mexico is the wind setup and the tide. As the transported water reaches the coastline, bottom friction slows its motion, causing the rise in the water level. For places such as United States East Coast with deep bathymetries wind setup is less, and therefore the resultant water level during a storm surge is also less. On the other hand, the Gulf of Mexico has a continental shelf with a low slope. Consequently, it has higher storm tide potential. Figure 4-1 shows storm surge inundation as a function of hurricane intensity on U.S. Saffir - Simpson wind scale for five bathymetries ranging from very deep to very shallow. As it can be observed there is a strong positive relationship between water level rise and storm category as well as the depth of continental shelf (Fitzpatrick 2014).

Storm tides caused by hurricanes pose the greatest risk to life and property. They can reach heights over 20 feet, travel several miles inland, and inundate hundreds of miles of coastline (NOAA 2020). Discussed earlier SLR trends and projections in Galveston, TX have the potential to make Harris County even more vulnerable to flooding by storm tides. Associated with climate change, projected increase in average tropical cyclone intensity could also contribute to elevated risk to storm tides in the future. According to Knutson et al. (2019), out of the various effects on storm surge, estimates of the magnitude and rates of future sea level rise most definitely expected to lead to higher average storm surge inundation in the 21st century. Therefore, social and economic consequences for low-lying and densely populated region of Harris County can be significant.

Several studies explored cumulative effects of sea-level rise and the changes in future tropical cyclone climate on storm surge risk (McInnes et al. 2003; Lin et al. 2012; Little et al. 2015; Garner et al. 2017; McInnes et al. 2014). While the increased storm surge inundation due to rising seas have been confirmed, the effect of the change in tropical cyclone activity remains uncertain and requires more research (Woodruff et al. 2013).

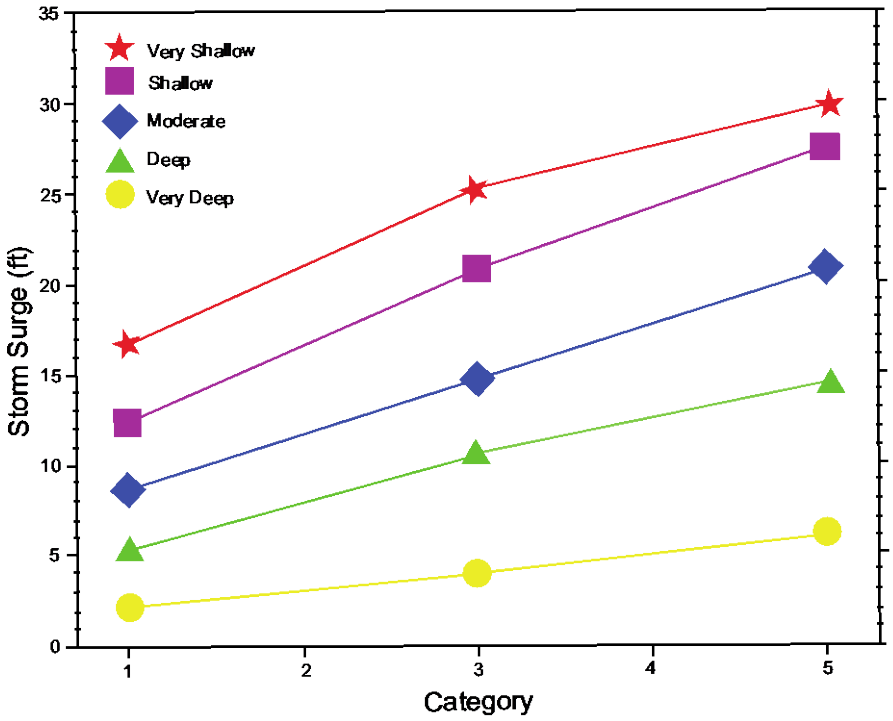

Figure 4-1 Storm surge relationship to ocean floor slope and hurricane intensity using the U.S. wind scale (modified after P. Fitzpatrick and Y. Lau 2011).

Combined Effect of Sea-Level Rise and Storm Tides

Neumann et al. (2009) states that higher sea level provides storm surges with a higher “launch point”, which may increase both the real extent and the depth of the surge. There are three prevailing methods for estimating the combined effect of sea-level change and storm surge flooding: numerical simulation that incorporates of SLR into a numerical model; a more linear approach that estimate the surge magnitude by superimposing SLR to storm surge heights; and a third method that considers quasilinear interaction between storm surge and SLR (Zhang et al. 2013). The later approach neglects the strong non-linear interaction between storm surge and sea-level that occurs in shallow waters. In addition, calculation of surge heights adjacent to

current inundation area becomes problematic. Because of this, linear addition by expansion has been employed to address these uncertainties. It is a more advanced linear superimposition method that accounts for spatial variability and provides the inundation area next to the current boundaries. Zhang et al. (2013) employs all three methods and compares them. The results show that there is a strong non-linear interaction between sea-level magnitude and storm surge heights in the coastal areas with low continental shelf. Zhang and colleagues also demonstrate that out of the three methods, simple linear addition tends to underestimate the flooded areas by 30% and water heights by 12%.

Bilskie and Hagen (2016), developed a dynamic modeling framework to examine the effects of SLR on storm surge. The concept behind this framework is that as global and regional sea-levels continue to rise in the changing climate, they alter coastal morphology, tides and marshes. In turn, these topographic changes alter the path, pattern, and magnitude of storm surge flooding. This innovative approach has resulted in a major paradigm shift from static models such as of Zhang et al. (2013) to dynamic ones. Bilskie and Hagen applied this methodology to the Northern Gulf of Mexico under four SLR scenarios for the year 2100. The result showed that inundated area increased by 87% and peak storm surge heights by as much as 3 ft. In the next chapter we present a geospatial framework for incorporation of SLR into storm surge modeling that provides a high-resolution inundation surface of storm surge under elevated sea-level condition for Harris County by 2100.

Model Description

Numerical models based on shallow water equations are employed for estimation of inundation due to storm tide. The SLOSH (Sea, Lake and Overland Surges from Hurricanes) is a highly efficient hydrodynamic numerical model for simulating storm surge. It was developed in the early 1980's by the Federal Emergency Management Agency (FEMA), United States Army Corps of Engineers (USACE) and the National Weather Service (NWS) for real time forecasting of hurricane storm surges (Jelesnianski et al. 1992). Although more sophisticated higher resolution storm surge models have been developed since, SLOSH continues to be used for operational forecasting within the NWS. This is mostly due to its extreme efficiency as it takes less than two minutes for a storm simulation while incorporating the essential physics. To ensure its accuracy for real-time surge forecasting, SLOSH model has been validated against historical and synthetic hurricanes with different intensities, sizes, moving speeds, and forward direction (Jelesnianski et al. 1992).

The SLOSH was developed as a two-dimensional (2D) finite difference code, which is also significantly reduces the time required for numerical computation. It is based on the 2D integrated shallow water equations and can be expressed using a Cartesian reference frame by

$$\frac{\partial U}{\partial t} = -g(D+h)\left[B_r \frac{\partial(h-h_0)}{\partial x} - B_i \frac{\partial(h-h_0)}{\partial y}\right] + f(A_r V + A_i U) + C_r x_\tau - C_i y_\tau$$

$$\frac{\partial V}{\partial t} = -g(D+h)\left[B_r \frac{\partial(h-h_0)}{\partial y} - B_i \frac{\partial(h-h_0)}{\partial x}\right] - f(A_r V + A_i U) + C_r y_\tau - C_i x_\tau$$

$$\frac{\partial h}{\partial t} = -\frac{\partial U}{\partial x} - \frac{\partial V}{\partial y}$$

with horizontal velocities of water masses (U, V), gravitational constant (g), depth of quiescent water relative to a common datum (D), height of water above datum (h), hydrostatic water height (h_0), Coriolis parameter(f), surface stresses (x_τ, y_τ), and bottom stress terms $(A_r, .. B_r, . C_i)$.

Methods

For this study, a geospatial framework was employed to generate an inundation surface for storm surge with sea-level rise (SLR) scenarios. Data from several sources were collected. These include data from U.S Geological Survey (USGS), National Hurricane Center (NHC), and NOAA's Office for Coastal Management.

The NHC uses SLOSH model for predicting storm surge heights. It has several products that range from forecasting surges for landfalling hurricanes to non-hurricane specific flooding that is used for long term planning and mitigation. For this study, it was most appropriate to use SLOSH data for non-hurricane specific flooding since the objective is to make projections for future sea-level scenarios. For that reason, the maximum of maximums envelopes of water (MOM) simulations were chosen. It is based on thousands of SLOSH simulations and used to produce the worst possible case scenario for a given hurricane category.

USGS offers elevation data from Digital Elevation Model (DEM) through their National Elevation Dataset (NED). The highest seamless resolution, 1/3 arc-second, DEM was downloaded through USGS's National Map service. Ground spacing for this

resolution is approximately 10 meters north/south, but variable east/west due to convergence of meridians with latitude.

Sea-level rise data is available through NOAA's Office of Coastal Management. Projected future sea-level data can be obtained for 0 to 6 feet scenarios in 1-foot increments. 2, 4, and 6 feet scenarios were utilized for this study.

In an effort to study the effect of future sea level rise on storm surge induced flooding in the Galveston basin, a geospatial model was executed to model four inundation surfaces for 0 (current conditions), 2, 4, and 6 ft sea-level rise scenarios. SLOSH Category 5 storm tide (with spring high tide) was used as the base case storm tide for the Galveston basin. To provide an assessment of the combined effects of sea-level rise and storm surge on the exposure and vulnerability of critical structures, data from the USGS Structures and Texas Department of Transportation (TxDOT) National Highway System (NHS) datasets were added to the modeled storm surge surfaces.

Results

Modeled Category 5 peak storm surge heights for the present condition and three sea-level rise scenarios for Galveston Bay and Harris County are shown in Figure 4-2. These modeled surfaces include the extent of permanently inundated areas due to SLR and storm surge inundation overland. Significant portion of Harris County is currently at risk of storm surge flooding from Category 5 hurricanes. Under current conditions, maximum storm surge of 25 feet occurs in the northern portion of the Bay. For Harris County maximum storm surge is observed in eastern portion of the county along the banks of the San Jacinto River. Modeled MOM for 2, 4, and 6 feet of SLR are

shown in the Figure 6b-6d. Apart from the permanently inundated land due to the SLR, maximum modeled surge values are predicted in the similar locations compared to the current scenario. The results demonstrate that the low-lying southeastern portion of the county is at most risk to storm surges under current and projected sea-levels. Although at risk areas are observed to experience varying levels of flooding due to SLR and storm surge, some locations are particularly vulnerable. In Harris County, these are the communities of Shoreacres, Taylor Lake Village, El Lago, and Seabrook. For adjacent Galveston County, communities of Bacliff and San Leon are also very vulnerable to storm surge flooding compounded by SLR. Flood inundation maps for 0, 2, 4, and 6 feet SLR scenarios show the change in storm surge heights as well as spatial variation of inundated area. As expected, both the magnitude and extent of surge induced inundation increased each time for three SLR cases. The greatest change in the extent and magnitude of flooding occurs between the present day and 6 feet SLR scenario.

The Galveston Bay area, specifically Harris County, is well developed and is a host to a variety of critical facilities such as healthcare, law enforcement, education, and government buildings. Other critical facilities include fire stations and post offices. Additionally, the Galveston Bay and Harris County is home to major economic activity supported by the infrastructure. To understand how SLR can potentially increase the vulnerability of people, structures and infrastructure to hurricane storm surge flooding, major highways and critical structures were overlaid with the modeled inundation surfaces. As can be seen in the Figure 4-3, Galveston-Houston area has an extensive highway network that plays a major role in the meeting this region’s mobility needs, supporting economy, and is crucial for evacuation and post-storm recovery operations.

SLR increases the exposure of this region's infrastructure to hurricane induced storm surge flooding. Accessibility of major highways is substantially decreased at the time of peak storm surge further increasing the vulnerability of this region. Under present conditions, Category 5 storm surge produces flooding of up 20 feet for portions of interstate highway I 45 and state highways Tx 6 and Tx 146 that serve as evacuation routes during hurricane events. Because automobiles are the main mode of transportation, accessibility of roads and highways during an evacuation event is vital and in some cases lifesaving. Magnitude and extent of inundation at locations of evacuation routes most exacerbated under 6 ft SLR scenario. Compounded by the effects of SLR, Category 5 hurricane induced storm surges pose an unprecedented, and possibly catastrophic risk of road closures.

Total amount of critical facilities inundated by storm surge under each sea-level scenario serves as an indicator of vulnerability of the study area. As demonstrated in Figure 4-4, structures outside of the extent of storm surge under current SLR conditions, are exposed to flooding under projected SLR due to amplifying effects of SLR. Number of inundated critical facilities increases as storm surge hazard zones are enhanced by projected sea-level scenarios. Count of flooded facilities in Harris county is 162 under present-day conditions, 249 with 2 ft SLR, 303 with 4 ft, and 370 with 6ft SLR. The total number of inundated structures increased by 128% from the present condition to the high scenario of 6 ft SLR.

Structures located in southeastern portion of Harris county are at the highest risk. For example, under present sea-level, El Lago City Hall is inundated by 11ft. Enhanced by 2, 4, and 6ft sea-level rise, the storm surge inundation levels increase to

16, 17, and 19 ft respectively. Inundation levels for Seabrook City Hall geographic location are 15, 20, 22, and 23 ft for the corresponding sea-level scenarios. This analysis shows that sea-level rise leads to the increase in the extent and magnitude of category 5 storm surges affecting Galveston Bay and Harris County. Observed changes in the flood-risk zones demonstrate the increase in vulnerability of the study area. Portions of Harris and Galveston counties located on the eastern side of Galveston Bay are the most vulnerable to the combined effects of sea-level rise and storm surge.

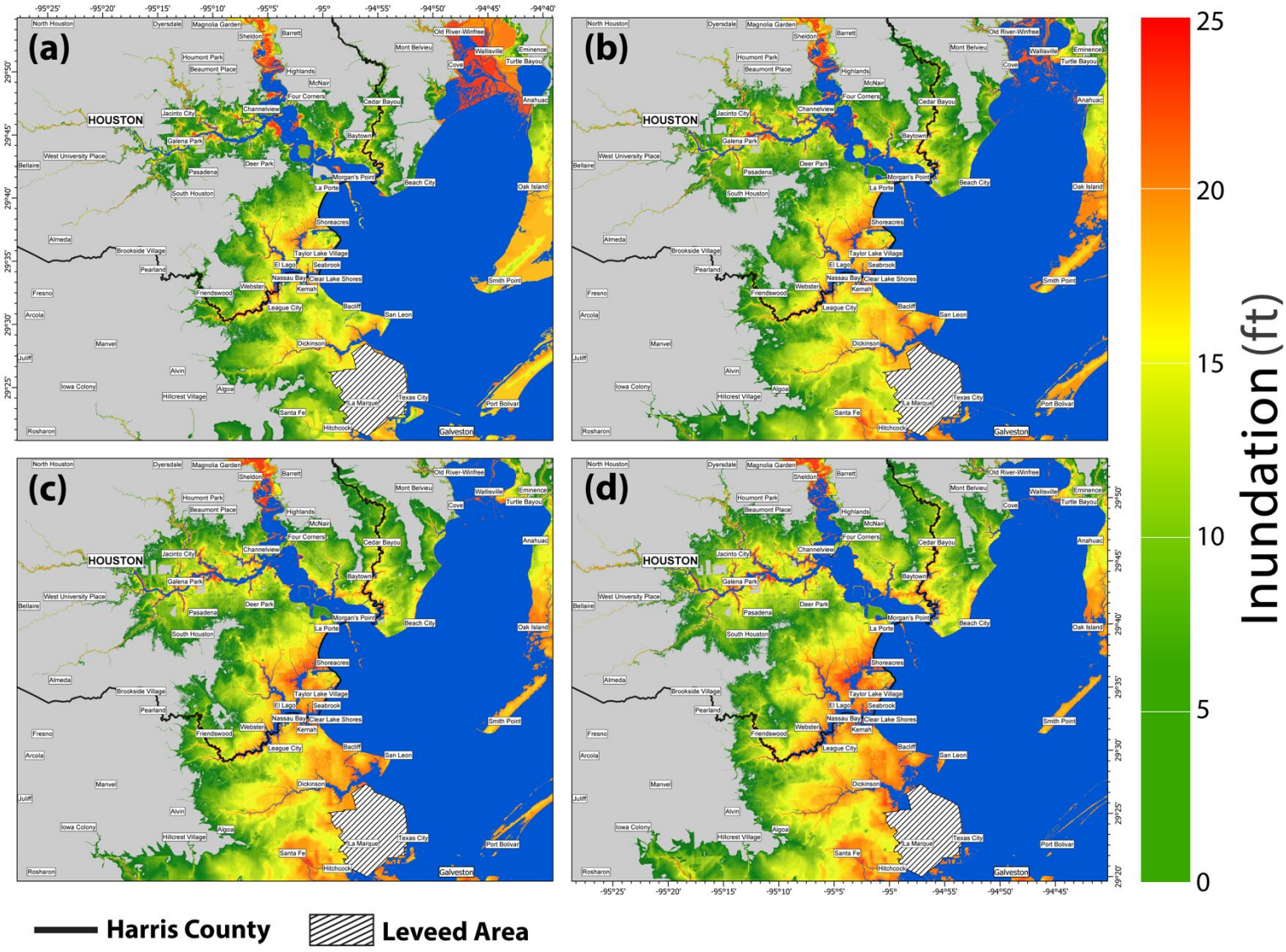

Figure 4-2 Modeled Category 5 storm tide with three sea-level rise (SLR) scenarios. **(a)** SLR 0 ft (current condition). **(b)** SLR 2 ft. **(c)** SLR 4 ft. **(d)** SLR 6 ft estimates from the USGCRP (2017) for 2100.

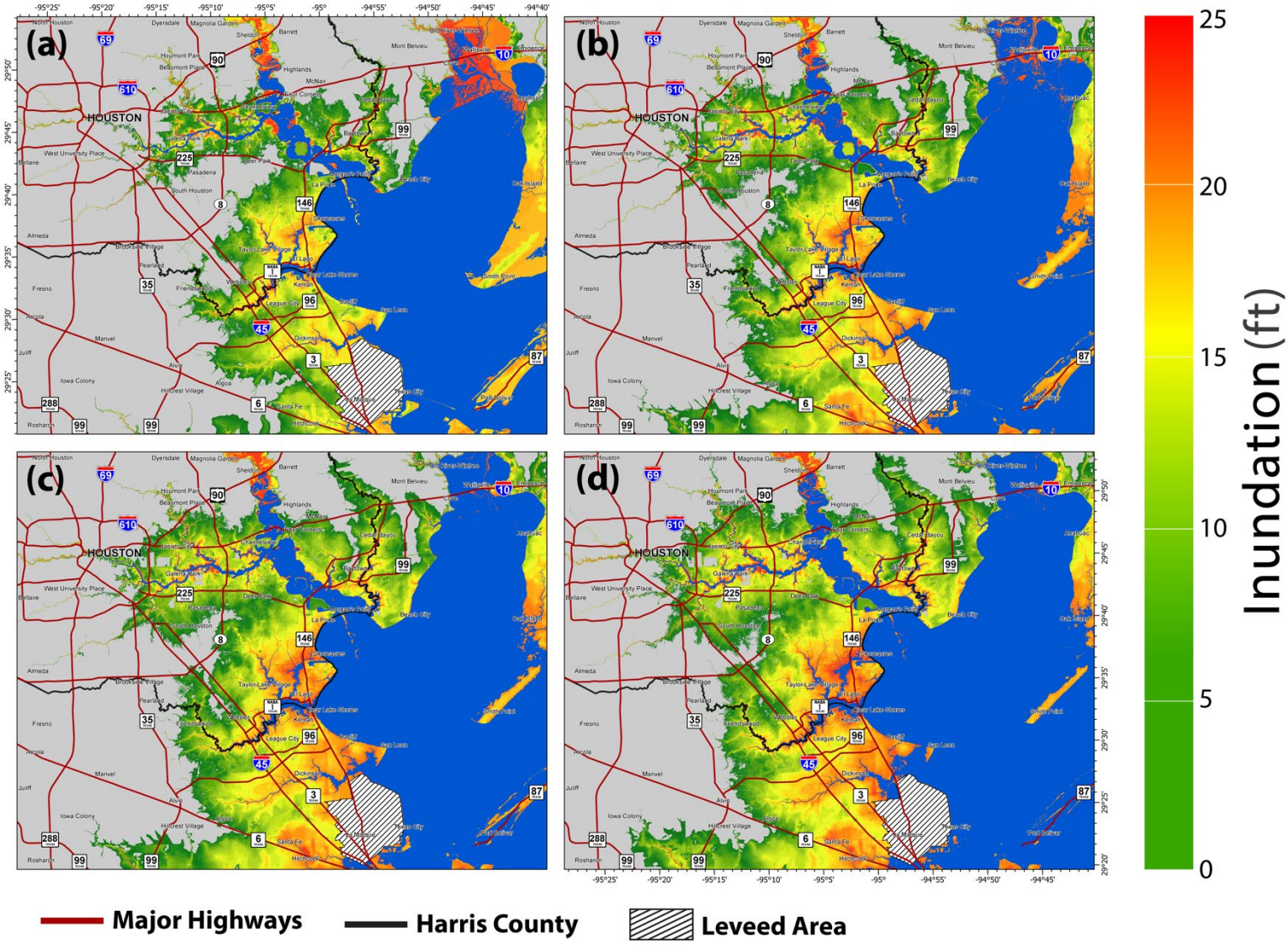

Figure 4-3 Modeled Category 5 storm tide with three SLR scenarios and major highways. **(a)** SLR 0 ft (current condition). **(b)** SLR 2 ft. **(c)** SLR 4 ft. **(d)** SLR 6 ft estimates from the USGCRP (2017) for 2100.

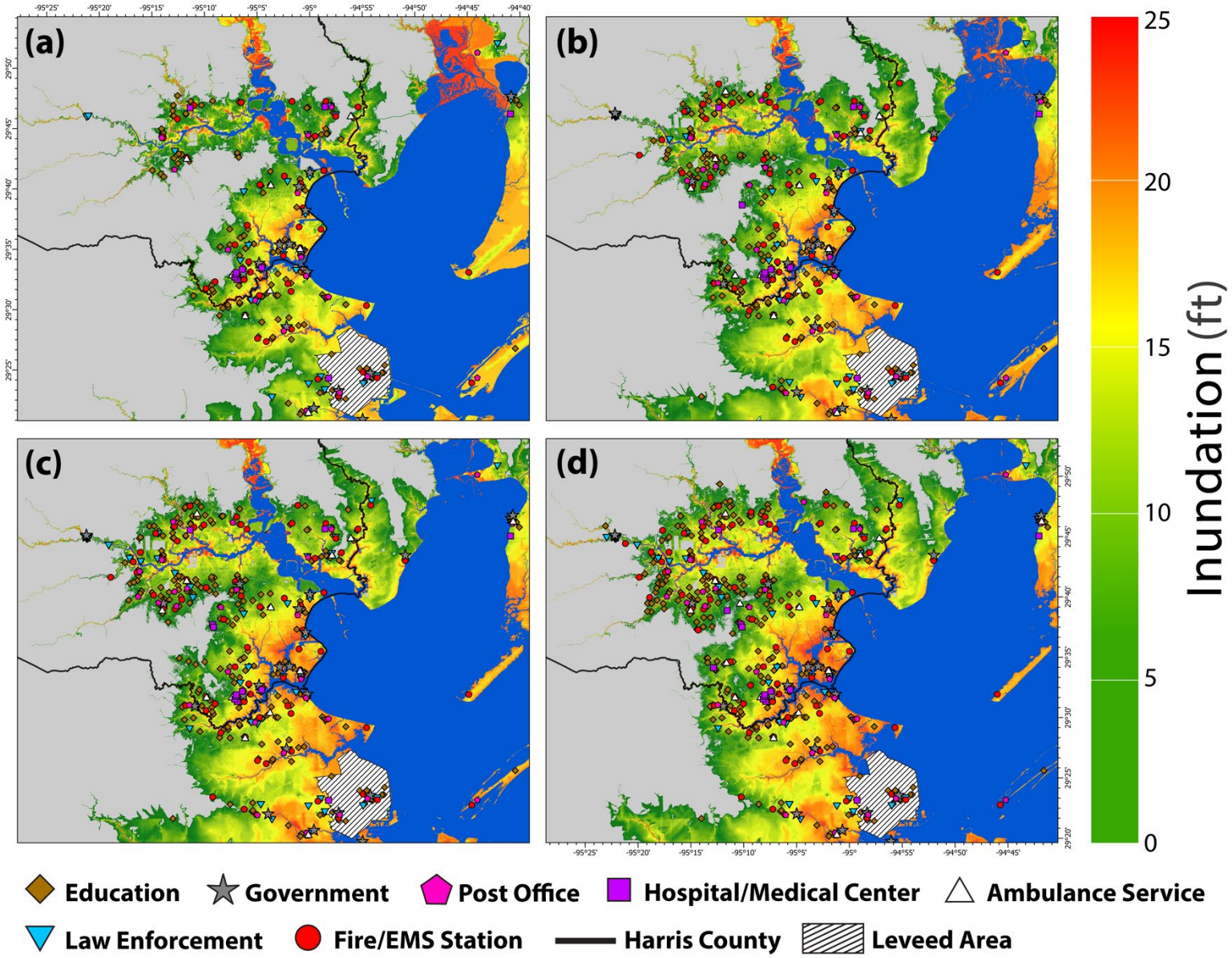

Figure 4-4 Modeled Category 5 storm tide with three SLR scenarios and critical structures. **(a)** SLR 0 ft (current condition). **(b)** SLR 2 ft. **(c)** SLR 4 ft. **(d)** SLR 6 ft from the USGCRP (2017) estimates for 2100.

CHAPTER 5

DISCUSSION AND CONCLUSIONS

This research represents an effort to analyze risk from storm tide and sea-level rise for a coastal region in the state of Texas. It supports a hypothesis of enhanced storm tide hazard zones due to sea-level rise in response to climate change. Storm surge impacts can include large-scale economic and environmental damage. In this study, the future flooding has been evaluated by the combined effects of climate change and hurricane induced storm tides. The approach relied on historical, observational and numerical model data, and involved statistical and geospatial modeling. Linear regression models are applied to tropical cyclone and tide-gauge data. Although these models are important, they have their limitations. Major hurricane counts for the Atlantic basin indicate a long-term upward trend. Some of the increasing frequency could be related to fluctuations in climate. Hurricane activity responds to changes in climate conditions including sea-surface temperatures, disturbances in the Trade winds, tropical waves, and wind shear. Thus, future research of hurricane flood hazards can include these climate variables.

For this study a geospatial framework is used for assessing risk and the impacts of climate change and SLR on local coastal flooding. This modeling approach incorporates projected SLR values into the SLOSH tidal surge projections from the National Hurricane Center and digital elevation models. Similar assessments of combined effects of SLR and storm tides on coastal flooding have been found to over and underestimate the magnitude and the extent of inundation. In a further approach, physical processes of hurricane driven storm surge and its complex interaction between

the sea floor, coastal erosion, and sea level rise need also be elaborated. Relative sea-level rise increases coastal regions vulnerability by enhancing storm surge hazard zones. Future studies can investigate the feasibility of reducing the vulnerability of the Southeastern portion of Texas coast to future storm tides under SLR and flood damages.

This study provides an initial assessment of hurricane flood hazards and the impacts of the interaction between sea-level rise and storm surges pertaining to the greater Houston area. A geospatial framework is proposed for modeling storm tide with sea-level rise. Spatial models and statistics are applied to the State of Texas with the focus on the Houston metropolitan area including Harris County. Historical and observational tropical cyclone data is used to examine past storm events and to construct spatial distribution models. The results of this study suggest that a greater amount of this region's infrastructure is projected to be exposed to damage from hurricane storm surge. Severe storm surges can damage infrastructure, hinder evacuation due to road closures and overwhelmed storm drains.

In the past decades Houston metropolitan area has experienced substantial population growth and development. Because Texas coastline has been one of the primary locations for crossing tropical storms and hurricanes, communities located in this region of Texas have been historically exposed to associated with them hazards. Climatology of tropical cyclones reveals increasing rates of hurricanes Category 3 and higher in the Atlantic basin. Spatial modeling of local tropical cyclone frequency and intensity in combination with population exposure demonstrates that Harris County is at high risk for hurricane hazards. Additionally, the after industrial trend in emissions from

human activities is estimated to cause record historic sea-level rise in the Galveston Bay under RCP 8.5. Climate change induced sea-level rise and increasing rates of intense hurricanes put the communities of Harris County at higher risk. Rising sea-levels along the Texas coast have already been slowly submerging low-lying areas, eroding beaches and causing nuisance flooding. SLOSH model simulations of Category 5 hurricane storm surges show that under present day sea-level, a significant portion of Harris County is at risk of storm surge flooding. Change in storm surges due to sea-level rise is one of the greatest impacts of warming climate. When combined with sea-level rise, magnitude and extent of flooding are amplified. Modeling of hurricane storm surge with projected sea-level rise scenarios shows that Harris County is extremely vulnerable to flooding under changing climate. There is a need to investigate the vulnerability of the population, highway infrastructure and critical structures and facilities to extreme hurricanes under rising sea level. An expected increase in the frequency of intense hurricanes and sea-levels would further exacerbate the vulnerability of this region. Under RCP 8.5, anthropogenic induced climate change is likely to substantially increase the vulnerability of people and infrastructure in greater Houston area to coastal flooding by 2100.

REFERENCES

Bilskie, M. V., S. C. Hagen, K. Alizad, S. C. Medeiros, D. L. Passeri, H. F. Needham, and A. Cox, 2016: Dynamic simulation and numerical analysis of hurricane storm surge under sea level rise with geomorphologic changes along the northern Gulf of Mexico. *Earth's Future*, **4**, 177–193, doi:10.1002/2015ef000347.

Bloemendaal, N., I. D. Haigh, H. D. Moel, S. Muis, R. J. Haarsma, and J. C. J. H. Aerts, 2020: Generation of a global synthetic tropical cyclone hazard dataset using STORM. *Scientific Data*, **7**, doi:10.1038/s41597-020-0381-2.

Church, J. A., and N. J. White, 2011: Sea-Level rise from the late 19th to the early 21st century. *Surveys in Geophysics*, **32**, 585–602, doi:10.1007/s10712-011-9119-1.

Church, J.A., P.U. Clark, A. Cazenave, J.M. Gregory, S. Jevrejeva, A. Levermann, M.A. Merrifield, G.A. Milne, R.S. Nerem, P.D. Nunn, A.J. Payne, W.T. Pfeffer, D. Stammer and A.S. Unnikrishnan, 2013: Sea Level Change. *Climate Change 2013: The Physical Science Basis. Contribution of Working Group I to the Fifth Assessment Report of the Intergovernmental Panel on Climate Change*. Cambridge University Press, Cambridge, United Kingdom and New York, NY, USA.

Delgado, S., C. W. Landsea, and H. Willoughby, 2018: Reanalysis of the 1954–63 Atlantic hurricane seasons. *Journal of Climate*, **31**, 4177–4192, doi:10.1175/jcli-d-15-0537.1.

Dolan, R. and H. Lins, 1985: The outer banks of North Carolina. *U.S. Geological Survey Professional Paper,* 1177-B.

Eggleston, J., and J. Pope, 2013: Land subsidence and relative sea-level rise in the southern Chesapeake Bay region. *U.S. Geological Survey Circular*, **1392**, 1–30, doi:10.3133/cir1392.

Elsner, J. B., and A. B. Kara, 1999: *Hurricanes of North Atlantics: Climate and Society*. Oxford University Press, 512 pp.

Elsner, J. B., J. P. Kossin, and T. H. Jagger, 2008: The increasing intensity of the strongest tropical cyclones. *Nature*, **455**, 92–95, doi:10.1038/nature07234.

Elsner, J. B., R. E. Hodges, and T. H. Jagger, 2011: Spatial grids for hurricane climate research. *Climate Dynamics*, **39**, 21–36, doi:10.1007/s00382-011-1066-5.

Emanuel, K., 1987: The dependence of hurricane intensity on climate. *Nature*, **326**, 483–485, doi:10.1038/326483a0.

Emanuel, K., 2011: Global warming effects on U.S. hurricane damage. *Weather, Climate, and Society*, **3**, 261–268, doi:10.1175/wcas-d-11-00007.1.

Emanuel, K., 2011: Global warming effects on U.S. hurricane damage. *Weather, Climate, and Society*, **3**, 261–268, doi:10.1175/wcas-d-11-00007.1.

Fitzpatrick, P. J., 2014: Tropical cyclones. *Encyclopedia of Natural Resources*. doi: 10.1081/E-ENRA-120047660.

Garner, A. J., and Coauthors, 2017: Impact of climate change on New York City's coastal flood hazard: Increasing flood heights from the preindustrial to 2300 CE. *Proc. Natl. Acad. Sci. USA*, 114, 11 861–11 866, https://doi.org/10.1073/pnas.1703568114.

Held, I. M., and M. Zhao, 2011: The response of tropical cyclone statistics to an increase in CO2 with fixed sea surface temperatures. *J. Climate*, **24**, 5353–5364, https://doi.org/10.1175/JCLI-D-11-00050.1.

IPCC, 2013*: Climate Change 2013: The Physical Science Basis. Cambridge University Press*, 1535 pp., https://doi.org/10.1017/CBO9781107415324.

Jagger, H., and J. B. Elsner, 2006: Climatology models for extreme hurricane winds near the United States. *Journal of Climate*, **19**, 3220–3236, doi:10.1175/jcli3913.1.

Jelesnianski, C. P., J. Chen, and W. A. Shaffer, 1992: SLOSH: Sea, lake, and overland surges from hurricanes. *NOAA Technical Report NWS 48, National Oceanic and Atmospheric Administration, U. S. Department of Commerce*, 71 pp.

Jevrejeva, S., A. Grinsted, and J. C. Moore, 2014: Upper limit for sea level projections by 2100. *Environmental Research Letters*, **9**, 104008, doi:10.1088/1748-9326/9/10/104008.

Kehew, A. E., 2017: *Geology for Engineers and Environmental Scientists*. Pearson Prentice Hall, pp. 595.

Keim, B. D., and R. A. Muller, 2009: *Hurricanes of the Gulf of Mexico*. Louisiana State University Press, Baton Rouge, 216 pp.

Klein, R.J.T. and R.J. Nicholls, 1998: Coastal zones. In: UNEP Handbook on Methods for Climate Change Impact Assessment and Adaptation Studies [Burton, I., J.F. Feenstra, J.B. Smith, and R.S.J. Tol (eds.)]. Version 2.0, United Nations Environment Programme and Institute for Environmental Studies, Vrije Universiteit, Amsterdam, The Netherlands, chapter 7, pp. 1–36.

Knapp, K. R., H. J. Diamond, J. P. Kossin, M. C. Kruk, C. J. Schreck, 2018: International best track archive for cclimate sstewardship (IBTrACS) pproject, vversion 4.NOAA National Centers for Environmental Information, doi.org/10.25921/82ty-9e16.

Knutson, T., and Coauthors, 2020: Tropical cyclones and climate change assessment: part II: Projected response to anthropogenic warming. *Bulletin of the American Meteorological Society*, **101**, doi:10.1175/bams-d-18-0194.1.

Kopp, R. E., and Coauthors, 2016: Temperature-driven global sea-level variability in the Common Era. *Proceedings of the National Academy of Sciences of the United States of America*, **113**, E1434–E1441, doi:10.1073/pnas.1517056113.

Kossin, J., T. Hall, T. Knutson, K. Kunkel, R. Trapp, D. Waliser, and M. Wehner, 2017: Ch. 9: Extreme Storms. Climate Science Special Report: Fourth National Climate Assessment. **1**, 257–276, doi:10.7930/j07s7kxx.

Landsea, C. W., and J. L. Franklin, 2013: Atlantic hurricane database uncertainty and presentation of a new database format. *Monthly Weather Review*, **141**, 3576–3592, doi:10.1175/mwr-d-12-00254.1.

Lin, N., K. Emanuel, M. Oppenheimer, and E. Vanmarcke, 2012: Physically based assessment of hurricane surge threat under climate change. *Nat. Climate Change*, **2**, 462–467, https://doi.org/10.1038/nclimate1389

Little, C. M., R. M. Horton, R. E. Kopp, M. Oppenheimer, G. A. Vecchi, and G. Villarini, 2015: Joint projections of US East Coast sea level and storm surge. *Nat. Climate Change*, **5**, 1114–1120, https://doi.org/10.1038/nclimate2801.

McInnes, K. L., K. J. E. Walsh, G. D. Hubbert, and T. Beer, 2003: Impact of sea-level rise and storm surges on a coastal community. *Nat. Hazards*, **30**, 187–207, https://doi.org/10.1023/A:1026118417752.

McInnes, K. L., K. J. E. Walsh, R. K. Hoeke, J. D. O'Grady, and F. Colberg, 2014: Quantifying storm tide risk in Fiji due to climate variability and change. *Global Planet. Change*, **116**, 115–129, https://doi.org/10.1016/j.gloplacha.2014.02.004.

Mctaggart-Cowan, R., E. L. Davies, J. G. Fairman, T. J. Galarneau, and D. M. Schultz, 2015: Revisiting the 26.5°C sea surface temperature threshold for tropical cyclone development. *Bulletin of the American Meteorological Society*, **96**, 1929–1943, doi:10.1175/bams-d-13-00254.1.

Moss, R. H., and Coauthors, 2010: The next generation of scenarios for climate change research and assessment. *Nature*, **463**, 747–756, doi:10.1038/nature08823.

Nerem, R. S., B. D. Beckley, J. T. Fasullo, B. D. Hamlington, D. Masters, and G. T. Mitchum, 2018: Climate-change–driven accelerated sea-level rise detected in the altimeter era. *Proceedings of the National Academy of Sciences*, **115**, 2022–2025, doi:10.1073/pnas.1717312115.

Neumann, J., K. Emanuel, S. Ravela, L. Ludwig, and C. Verly, 2015: Risks of coastal storm surge and the effect of sea level rise in the Red River Delta, Vietnam. *Sustainability*, **7**, 6553–6572, doi:10.3390/su7066553.

NOAA, 2020: National Oceanic and Atmospheric Administration, Tides and Currents. Accessed 1 February 2020, https://tidesandcurrents.noaa.gov/stations.html?type=Water+Levels.

NOAA, 2020: Re-Analysis Project. Accessed 1 February 2020, https://www.aoml.noaa.gov/hrd/hurdat/Data_Storm.html.

Smith, K., 2011: We are seven billion. *Nature Climate Change*, **1**, 331–335, doi:10.1038/nclimate1235.

Sugi, M., H. Murakami, and J. Yoshimura, 2012: On the mechanism of tropical cyclone frequency changes due to global warming. *J. Meteor. Soc. Japan*, **90A**, 397–408,

Sweet, W. V., R. E. Kopp, C. P. Weaver, J. Obeysekera, R. M. Horton, E. R. Thieler, and C. Zervas, 2017: Global and regional sea level rise scenarios for the United States (NOAA Technical Report NOS CO-OPS 083). *Washington, DC: Center for Operational Oceanographic Products and Services National Ocean Service, National Oceanic and Atmospheric Administration*.

USGCRP, 2017: *Climate Science Special Report: Fourth National Climate Assessment, Volume I* [Wuebbles, D.J., D.W. Fahey, K.A. Hibbard, D.J. Dokken, B.C. Stewart, and T.K. Maycock (eds.)]. U.S. Global Change Research Program, Washington, DC, USA, 470 pp, doi: 10.7930/J0J964J6. Vigh, J. L., E. Gilleland, C. L. Williams, D. R. Chavas, N. M. Dorst, 2016: TC-OBS: The tropical cyclone observations-based structure database (version 0.42, an alpha-level release). Tropical Cyclone Data Project, National Center for Atmospheric Research, Research Applications Laboratory, Boulder, Colorado. http://dx.doi.org/10.5065/D6BC3X95.

Wallace, J. M., and P. V. Hobbs, 2011: *Atmospheric Science: An Introductory Survey*. Elsevier Acad. Press, 483 pp.

Walsh, K. J. E., and Coauthors, 2015: Hurricanes and climate: The U.S. CLIVAR working group on hurricanes. *Bull. Amer. Meteor. Soc*., **96**, 997–1017, https://doi.org/10.1175/BAMS-D-13-00242.1.

Wheeler, S., and T. Beatley, 2017: *The Sustainable Urban Development Reader*. Routledge, 939 pp.

Woodruff, J. D., J. L. Irish, and S. J. Camargo, 2013: Coastal flooding by tropical cyclones and sea level rise. *Nature*, **504**, 44 - 52, https://doi.org/10.1038/nature12855.

Xu, N., 2018: Detecting coastline change with all available landsat data over 1986–2015: a case study for the State of Texas, USA. *Atmosphere*, **9**, 107, doi:10.3390/atmos9030107.

Yoshimura, J., and M. Sugi, 2005: Tropical cyclone climatology in a high-resolution AGCM—Impacts of SST warming and CO2 increase. *SOLA*, **1**, 133–136, https://doi.org/10.2151/sola.2005-035.

Zhang, K., Y. Li, H. Liu, H. Xu, and J. Shen, 2012: Comparison of three methods for estimating the sea level rise effect on storm surge flooding. *Climatic Change*, **118**, 487–500, doi:10.1007/s10584-012-0645-8.

Zhao, M., and Coauthors, 2013: Robust direct effect of increasing atmospheric CO2 concentration on global tropical cyclone frequency: A multi-model inter-comparison. *US CLIVAR Variations*, Vol. **11**, No. 3, US CLIVAR Project Office, Washignton, DC, 17–23,